MECHANISTIC STUDIES ON THE REACTION OF COB(I)ALAMIN AND NITRITE

A thesis submitted to the
Kent State University Honors College
in partial fulfillment of the requirements
for University Honors

by

Noah Plymale

May, 2011

TABLE OF CONTENTS

LIST OF FIGURES

LIST OF SCHEMES

LIST OF TABLES

ACKNOWLEDGEMENTS

I would like to thank my advisor Dr. Nicola Brasch for all of her support and guidance along the way. She was instrumental in making this experience a good one. I would also like to thank my graduate mentor, Dr. Hanaa Hassanin for helping me get started. I would also like to thank my thesis committee, Dr. Doug Kline, Dr. Brett Ellman, and Dr. Edwin Gould. I am extremely grateful to the Brasch Lab, Dr. Riya Mukherjee, Harishchandra Subedi, Rohan Dassanayake, Jeffery Brown, David Walker, and Brian Smith. Finally, I would like to acknowledge and thank the NSF for funding this work and making this experience possible.

I. INTRODUCTION

Reactive molecules can pose many problems in the delicate balance of biological systems. Of particular importance are reactive oxygen species (ROS) and reactive nitrogen species (RNS) that can cause cellular oxidative and nitrosative stress. The most abundant ROS include superoxide ($O_2^{\bullet-}$), hydrogen peroxide (H_2O_2), and hydroxyl radical ($HO^{\bullet-}$) and RNS include $NO_2^{\bullet}$, ONOO(H), and NO_2^-.[1-3]

$^{\bullet}$NO is produced from L-arginine, which is enzymatically converted to L-citrulline by nitric oxide synthase.[4-6] $^{\bullet}$NO is an important signaling molecule in biology that is implicated in vasodilation and neurotransmission at nanomolar (nM) concentrations.[7] Additionally, higher concentrations of $^{\bullet}$NO are known to occur as part of the immune response to inflammation caused by infection.[8,9] $^{\bullet}$NO is oxidized to NO_2^-, which can be further oxidized to NO_3^-. The production of NO_2^- and NO_3^- is used as an indicator of the production of $^{\bullet}$NO.[10-14] NO_2^- concentrations are high in plasma and tissue, which, under normal conditions, contain up to 0.5 and 10 μM NO_2^- respectively.[8,15] During sepsis, serum levels of NO_3^- and NO_2^- are significantly elevated.[16] NO_2^- may also be produced by the reduction of NO_3^-, which is present in significantly higher quantities than NO_2^- or $^{\bullet}$NO.[17] NO_3^- is reduced by mammalian enzymes possessing nitrate reductase activity or by bacteria in the mouth and intestines possessing nitrate reductase.[8] Indeed, mounting evidence suggests that NO_2^- may function as a biological signaling molecule and play an important role in vasodilation and intravascular endocrine $^{\bullet}$NO transport.[18]

Vitamin B_{12} derivatives, known as cobalamins (Cbl), are essential nutrients synthesized only by microorganisms and obtained by higher organisms through the diet.[19,20] The three biologically relevant oxidation states of cobalamins are Cbl(I), Cbl(II), and Cbl(III), in which the cobalt metal center is in the +1, +2, and +3 oxidation state, respectively. Oxidation-reduction processes play an important role in the biochemistry of cobalamin.[21] Insufficient Cbl in the metabolism is associated with neurological disorders and pernicious anemia.[19] The general structure of Cbl(III) (Figure 1) consists of an octahedral cobalt center coordinated to a corrin ring, a nucleotide base, and any of a

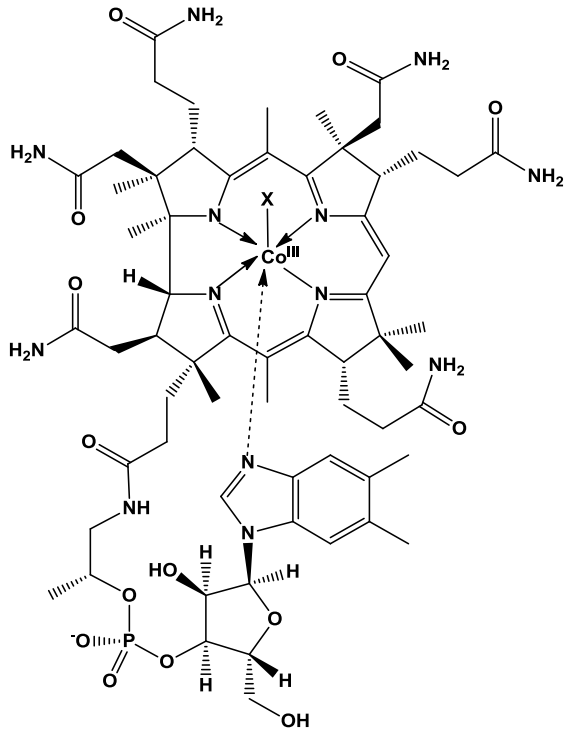

Figure 1: Structure of cob(III)alamins. The β-axial site (indicated by the X) can be occupied by a variety of ligands. X = CN: cyanocobalamin; CH_3: methylcobalamin (CH_3Cbl); 5'-deoxyadensosyl: adenosylcobalamin (AdoCbl); H_2O: aquacobalamin; HO^-: hydroxocobalamin (HOCbl); NO: nitrosylcobalamin; NO_2: nitrocobalamin; glutathione: glutathionylcobalamin.[20,21]

variety of ligands in the upper β-axial position. The major form of cobalamin found in cells is the oxygen-sensitive, pentacoordinate Cbl(II) complex, which lacks the ligand in the upper β-axial site.[21,22] Cbl(I), which is far more sensitive to oxidation than Cbl(II), lacks both axial ligands. Hence, changes in oxidation states of cobalamin is accompanied by changes in the number of axial ligands associated with the complex.[21]

There are two well-characterized B_{12}-dependent enzyme reactions in mammals, which involve cycling of the Cbl oxidation state. The first utilizes adenosylcobalamin (AdoCbl) as an enzyme cofactor in the methylmalonyl-CoA mutase (MMCM) reaction (Scheme 1). The Cbl is cycled between AdoCbl with the 5'-deoxyadenosyl bound to the cobalt at the β-axial site and Cbl(II) with the 5'-deoxyadenosyl unbound.[20,21] The methionine synthase reaction is the other B_{12}-dependent reaction in mammals (Scheme 2). The Cbl cycles between methylcobalamin (CH_3Cbl) and Cbl(I), catalyzing the transfer of a methyl group from methyltetrahydrofolate to homocysteine to form the amino acid methionine.[20] Cbl(I) very easily oxidized to Cbl(II), and under microaerophilic conditions it is known that for ~2000 turnovers of the methionine synthase catalytic cycle, Cbl(I)

Scheme 1: L-methylmalonyl-CoA is isomerized to succinyl-CoA by the AdoCbl-dependent enzyme methylmalonyl-CoA mutase (MMCM). The Cbl cycles between AdoCbl and Cbl(II).[20,21]

undergoes oxidation to Cbl(II).[20,21] In order to complete the cycle, Cbl(II) must then be reduced by flavodoxin prior to methyl donation from *S*-adenosylmethionine to reform CH_3Cbl (Scheme 2).

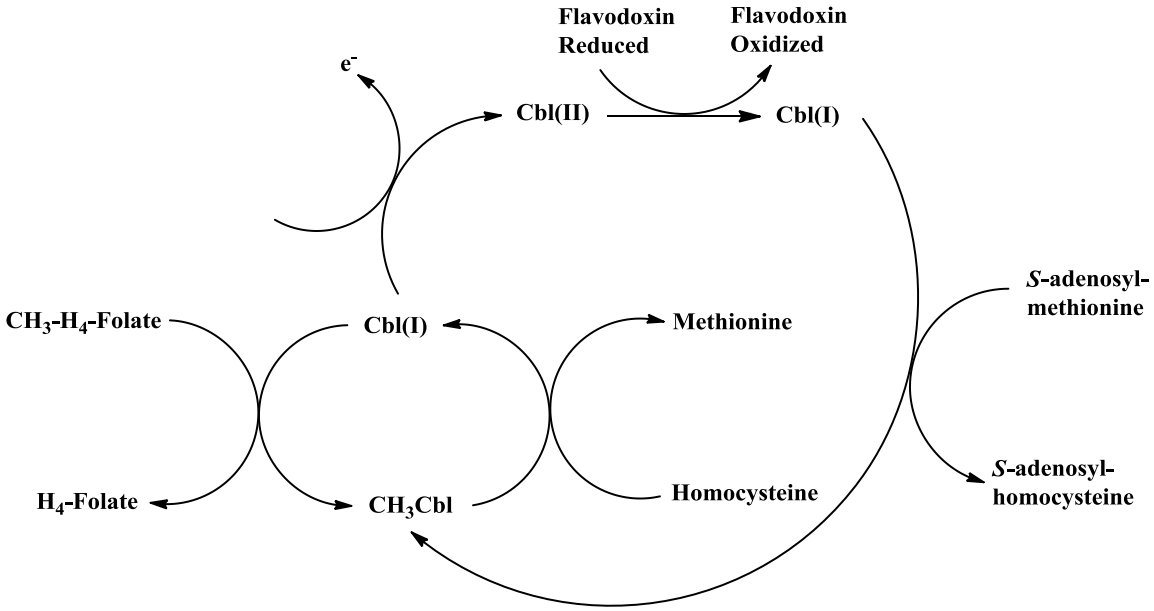

Scheme 2: The B_{12}-dependent methionine synthase reaction, in which methyltetrahydrofolate methylates homocysteine to give methionine. The process involves the cycling of Cbl between CH_3Cbl and Cbl(I). Under microaerophilic conditions, Cbl(I) is oxidized to Cbl(II) every ~2000 enzyme turnovers. Reactivation involves flavodoxin, *S*-adenosylmethionine, and methionine synthase reductase.[20]

Cbl is taken up and transported by three B_{12} binding proteins – intrinsic factor (IF), transcobalamin (TC), and haptocorrin (HC).[21] These proteins are associated with membrane receptor proteins that allow intracellular uptake of the B_{12} to ultimately deliver it to the methionine synthase and MMCM enzymes. Chronic inflammation is associated with elevated levels of TC[23] and its membrane receptor.[24] Thus, B_{12} is thought to

participate in the cellular response to inflammation. It has also been suggested that B_{12} has antioxidant properties in part because of its ability to regulate cytokines.[25]

ROS and RNS are implicated in numerous diseases and health conditions, including septic shock, ischemic / reperfusion injury, atherosclerosis, and asthma.[26-29] These conditions are generally associated with inflammation. Oxidative stress is known to produce a cellular redox imbalance, a common occurrence in several types of cancer.[30] Additionally, megaloblastic anemia is associated with elevated levels of $^{\bullet}NO$,[31] and plasma levels of NO_2^- and NO_3^- are reportedly significantly elevated in patients with vitiligo,[32] a skin pigmentation disorder. It has been reported that vitamin B_{12} can restore normal levels of $^{\bullet}NO$ in patients with megaloblastic anemia.[31]

In addition to playing a key role in the methionine synthase reaction, Cbl(I) is a transient intermediate in the biosynthesis of both CH_3Cbl and AdoCbl.[20] Importantly both mammalian B_{12}-dependent enzyme reactions are inactivated under oxidative / nitrosative stress conditions.[33] The purpose of this study is to determine whether oxidation of Cbl(I) by the RNS NO_2^- could occur under oxidative / nitrosative stress conditions. The mechanism and rate constants of the reaction of Cbl(I) with NO_2^- / HNO_2 have been determined by studying the kinetics of the reaction under varying conditions, determining the reaction stoichiometry, and elucidating the Cbl and non-Cbl products of the reaction.

II. EXPERIMENTAL SECTION

2.1 Chemicals

Hydroxycobalamin hydrochloride, HOCbl·HCl(·nH_2O) (≥ 96%, 10-15% water, batch dependent) was purchased from Fluka. BIS-TRIS and TAPS buffers were purchased from Sigma. Sodium borohydride ($NaBH_4$, ≥ 98%), anaerobic acetone (99.8%), CAPS, CHES, and MES buffer, sodium nitrite ($NaNO_2$, 99.6%), sodium hydroxide (NaOH), and hydroxylamine hydrochloride ($NH_2OH·HCl$, ≥ 97%) were purchased from Acros. Disodium hydrogen phosphate (Na_2HPO_4), sodium dihydrogen phosphate (NaH_2PO_4), sodium carbonate (Na_2CO_3), potassium cyanide (KCN, ≥ 99.1%), and 8-hydroxyquinoline (≥ 99%) were purchased from Fisher Scientific. Nessler reagent was purchased from RICCA Chemical. Water was purified using a Barnstead Nanopure Diamond water purification system.

2.2 Instrumental and Procedures

For all Cbl(I) experiments, anaerobic solutions were degassed by four freeze-pump-thaw cycles under argon gas using standard Schlenk techniques. Solutions prepared for Cbl(II) work were degassed by bubbling through argon for at least 2 hr. Preparation of all anaerobic solutions was carried out in an MBRAUN Labmaster 130 (1250/78) Glove box filled with argon, equipped with O_2 and H_2O sensors and a freezer at -24 °C. The pH measurements were done at room temperature using an Orion model

710A pH meter equipped with Mettler-Toledo Inlab 423 or 421 pH electrodes. The electrode was filled with a 3 M KCl / saturated AgCl solution (pH 7.0) and standardized with standard buffer solutions at pH 4.00, 7.00, 10.00, and 12.45. Solution pH was adjusted using H_3PO_4 or NaOH solutions as necessary.

Ultraviolet-visible (UV-Vis) spectroscopy data were recorded on a Cary 5000 spectrophotometer equipped with a thermostated (25.0 ± 0.1˚C) cell changer operating with WinUV Bio software (version 3.00). Kinetic data for fast reactions were collected under strictly anaerobic conditions at 25.0 ± 0.1˚C using an Applied Photophysics SX20 stopped-flow spectrophotometer equipped with a photodiode array detector in addition to a single wavelength detector, with single-mixing capabilities. A continuous flow of nitrogen was used to maintain anaerobic conditions. Data was collected with Pro-Data SX (version 2.1.4) and Pro-Data Viewer (version 4.1.10) software, and a 1.0 cm pathlength cell was utilized. Data was analyzed using Microcal Origin version 8.0.

2.3 Synthesis of Cbl(I)

Cbl(I) was synthesized under anaerobic conditions according to a modified published procedure.[34] HOCbl·HCl (~25 mg, 1.6 x 10^{-5} mol (10-15 % H_2O)) was dissolved in anaerobic water (0.75 ml) in a vial. An aqueous, anaerobic stock solution of $NaBH_4$ (~10 mg, 2.6 x 10^{-4} mol, 1.00 mL) was prepared and $NaBH_4$ (6.0 mole equiv.) was added to the HOCbl·HCl. The vial was shaken vigorously for ~1 min and the reaction was allowed to occur for an additional 15 min. After the reaction was complete, the excess $NaBH_4$ was quenched by addition of acetone (0.200 mL) except when noted

otherwise. Note that for all experiments performed with the stopped-flow instrument, the excess $NaBH_4$ was not quenched in order to provide added stability to the Cbl(I) reagent solution. The product was characterized by UV-Vis spectrophotometry (λ_{max} 280, 288, 386, 455, 545, 680 nm[35]) (Figure 2) and stored under anerobic conditions at -24 °C.

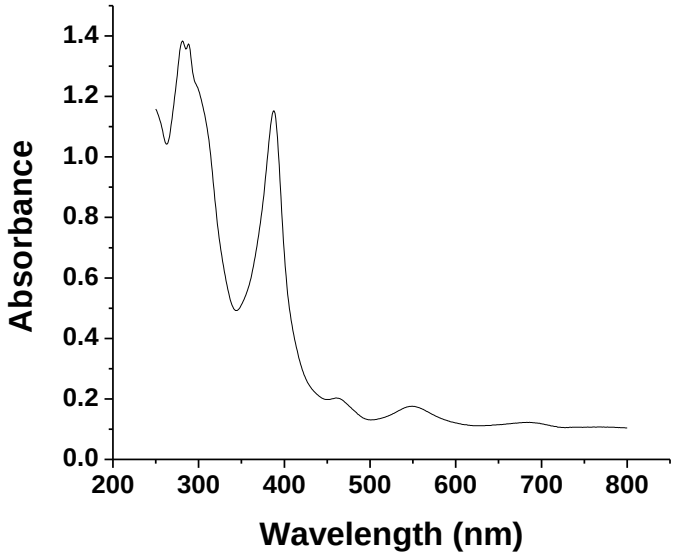

Figure 2: UV-Vis spectrum of Cbl(I) (50 μM) in anaerobic water (250 – 800 nm).

2.4 Synthesis of Cbl(II)

Cbl(II) was synthesized under anaerobic conditions according to a modified published procedure.[34] HOCbl·HCl (~25 mg, 1.6 x 10^{-5} mol (10-15 % H_2O)) was dissolved in anaerobic water (0.75 ml) in a vial under anaerobic conditions. An aqueous, anaerobic stock solution of $NaBH_4$ (~5 mg, 2.6 x 10^{-4} mol, 1.00 mL) was prepared and $NaBH_4$ (1.1 mole equiv.) was added to the HOCbl·HCl solution. The vial was shaken vigorously for ~1 min and the reaction was allowed to occur for an additional ~20 min.

Cbl(II) was characterized by UV-Vis spectrophotometry (λ_{max} 267, 285, 315, 467 nm[35]) (Figure 3), and solutions were stored under anaerobic conditions at -24 °C.

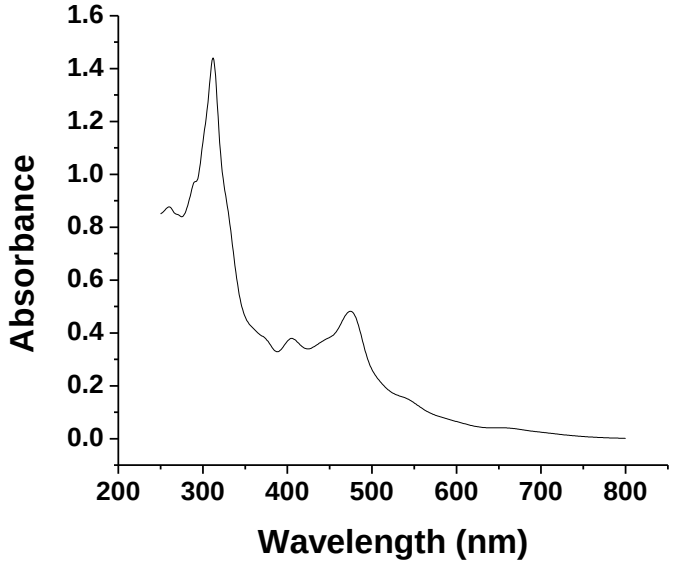

Figure 3: UV-Vis spectrum of Cbl(II) (50 µM) in anaerobic water (250 – 800 nm).

2.5 Determining Cobalamin Concentrations

The concentration of cobalamin in stock solutions was determined by converting the cobalamins to dicyanocobalamin, $(CN)_2Cbl^-$, with cyanide. Unless otherwise stated, the concentration determination was performed in triplicate under aerobic conditions, in order to convert all cobalamin species to $(CN)_2Cbl^-$. The reaction was allowed to occur for at least 2 hr and the stock solution was diluted for analysis by UV-Vis spectrophotometry. It was found that performing six replicate dilutions and allowing the reaction to occur over ~3 hr improved precision of the results. Additionally, maintaining dilution ratios less than 1:10 improved precision as well. UV-Vis spectra (250 – 800 nm)

were collected, and the absorbance at 368 nm was used to determine the concentration of the stock solution (ε_{368} = 3.04 x 10^4 $M^{-1}cm^{-1}$ for $(CN)_2Cbl^-$ [36]).

2.6 Attempts to Stabilize Cbl(I) by Precipitation

Cbl(I) was synthesized according to the procedure in Section 2.3. The product Cbl(I) stock solution was added drop wise to chilled acetone (~20 mL, -24 ˚C). The resulting precipitate was filtered using vacuum filtration on a microporous frit in the glove box. Attempts were also made to synthesize solid Cbl(I) by evaporating the solvent to dryness under vacuum on a Schlenk line. The solid Cbl(I) products were characterized by re-dissolving in water and obtaining a UV-Vis spectrum.

2.7 Determination of the Cbl Product of the Reaction of Cbl(I) with Nitrite

A phosphate buffer (0.050 M, pH 12.00) and a phosphate buffer containing $NaNO_2$ (30.03 mM) were prepared. Cbl(I) was synthesized according to the procedure described in Section 2.3 and the concentration (0.0122 M) was estimated by assuming the HOCbl·HCl contained 12 % H_2O. Cbl(I) (50 µM) was reacted with NO_2^- (9.1 mM) in an anaerobic Schlenk cuvette, and UV-Vis spectra were collected every 2.5 min for a total of 40 min. The cuvettes used were equipped with a cavity where the Cbl(I) reagent was stored so the reactants could be combined immediately before beginning data collection.

2.8 Determining the Stoichiometry of the Reaction between Cbl(I) and Nitrite

The stoichiometry of the Cbl(I) + NO_2^- reaction was determined in anaerobic CHES buffer (5.0 x 10^{-3} M, pH 9.51). A solution containing $NaNO_2$ (2.96 x 10^{-4} M) in CHES buffer (5.0 x 10^{-3} M, pH 9.51) was prepared. Cbl(I) was synthesized by dissolving HOCbl·HCl (50.26 mg) in anaerobic water (1.50 mL) and adding aqueous, anaerobic $NaBH_4$ (0.318 M, 0.608 mL, 6.0 mole equiv.) with shaking for ~1 min. The reaction was allowed to occur for ~15 min and excess $NaBH_4$ was quenched with anaerobic acetone (0.200 mL). The Cbl(I) concentration was determined by conversion to $(CN)_2Cbl^-$ (Section 2.5). This was performed in triplicate, diluting 50.0 µL, 100 µL, and 150 µL of cobalamin stock solution to 1.00 mL, 1.00 mL, and 2.00 mL respectively with aqueous 0.10 M KCN. The reaction was allowed ~2 hr to take place. The Cbl(I) concentration was determined to be (1.29 ± 0.06) x 10^{-2} M.

The Cbl(I) solution was combined with NO_2^- solution in CHES buffer under anaerobic conditions. Cbl(I) (200 ± 9 µM) was added to solutions containing varying mole equiv. of NO_2^- (0.050, 0.10, 0.15, 0.20, 0.25, 0.30, 0.35, 0.40, 0.45, and 0.50). The minimal time required for each reaction to proceed to completion was determined to be ~30 min by observing the time required for the spectrum of the solution containing Cbl(I) with 0.050 mole equivalents of NO_2^- to come to equilibrium. UV-Vis spectra for each solution were collected from 250 – 800 nm. Absorbance versus equiv. of NO_2^- plots were generated at 500 nm and 700 nm.

A second trial of the experiment was performed in a similar manner with some minor modifications. Cbl(I) was synthesized following the same general procedure by

dissolving HOCbl·HCl (100.31 mg) in 3.0 mL of anaerobic water and adding aqueous, anaerobic $NaBH_4$ (1.469 mL, 0.261M, 6.0 mole equiv.). The reaction was allowed to proceed as before and acetone (0.200 mL) was added. The Cbl(I) concentration was determined according to the protocol described in Section 2.5. Six replicate dilutions of 0.500 mL Cbl(I) stock solution to 5.00 mL with aqueous, aerobic KCN (0.100 M) were performed followed by two 1:10 dilutions (0.200 mL to 2.00 mL and 0.500 mL to 5.00 mL, sequentially). After completion of the stoichiometry experiment, 3 additional replicates for the determination of the Cbl(I) concentration were completed to confirm the Cbl(I) concentration by following a slightly altered dilution protocol. First, 1.00 mL Cbl(I) solution was diluted with 1.00 mL of anaerobic water and 3 samples of 0.500 mL of this solution were subsequently diluted to 5.00 mL with aerobic KCN (0.100 M). Subsequent dilutions (0.200 mL to 2.00 mL and 1.00 mL to 5.00 mL, sequentially) were performed using KCN (0.100 M). Each dilute solution was allowed to react for ~2 hr and UV-Vis spectra were recorded from 250 – 800 nm. The absorbance at 368 nm was used as before to determine the concentration of the original stock Cbl(I) solution, giving (1.25 ± 0.05) x 10^{-2} M. The Cbl(I) solution was diluted with equal parts of anaerobic water to give a final Cbl(I) concentration of (6.2 ± 0.3) x 10^{-3} M. The stoichiometry experiment was carried out as described above.

The stoichiometry of the reaction of Cbl(I) and NO_2^- was also determined at pH 7.40 (5.0 x 10^{-3} M phosphate buffer). An aqueous, anaerobic $NaNO_2$ (6.39 x 10^{-4} M) solution was prepared in the phosphate buffer. The same general procedure was followed as for the stoichiometry experiment at pH 9.53. The Cbl(I) concentration was determined

by performing six replicate dilutions of 0.500 mL Cbl(I) stock solution to 5.00 mL with aqueous, aerobic KCN (0.100 M) (Section 2.5). Each replicate solution was further diluted 1:10 (0.500 mL diluted to 5.00 mL) and then 1:5 (1.00 mL diluted to 5.00 mL). Additionally, this reaction was carried out for ~3 hr to assure reaction completion. The Cbl(I) concentration was determined as described previously to give $(1.22 \pm 0.02) \times 10^{-2}$ M. The stoichiometry experiment was performed as described above.

A replicate of the stoichiometry experiment at pH 7.40 was performed using separately prepared phosphate buffer (5.0×10^{-3} M, pH 7.40) and $NaNO_2$ (5.07×10^{-4} M in phosphate buffer) solutions. The Cbl(I) concentration was determined in the same way as for the previous replicate, giving $(1.24 \pm 0.03) \times 10^{-2}$ M. The stoichiometry experiment was performed according to the same procedure described above.

2.9 Determining the Amount of Hydroxylamine Product Formed: Indooxine Test

A modified literature procedure[37] (indooxine test) was used to determine the amount of NH_2OH produced by the reaction of Cbl(I) and NO_2^-. Aqueous $NH_2OH{\cdot}HCl$ standard solutions (25.00 mL) of varying concentrations (0, 20.0, 40.0, 50.0, 60.0, 80.0, and 100 μM) were prepared by diluting a stock $NH_2OH{\cdot}HCl$ solution (10.0 mL, 3.42×10^{-3} M). An 8-hydroxyquinoline solution (25.00 mL, 4.0 % w/v) was prepared in pure ethanol with stirring (~2 min). This concentration was found to be optimum for the assay. An aqueous Na_2CO_3 solution (100 mL, 1.00 M) was prepared. Calibration standards were prepared by the addition of 8-hydroxyquinoline (1.00 mL, 4.0 % w/v) to 1.00 mL of an NH_2OH solution of a specific concentration, followed by the addition of Na_2CO_3 (1.00

mL, 1.00 M). The reaction was allowed to proceed for 15 min and absorbance spectra for the standards were subsequently measured from 450 – 800 nm. The absorbance at 710 nm was plotted against the concentration of NH_2OH. The calibration curve is shown in Figure 4.

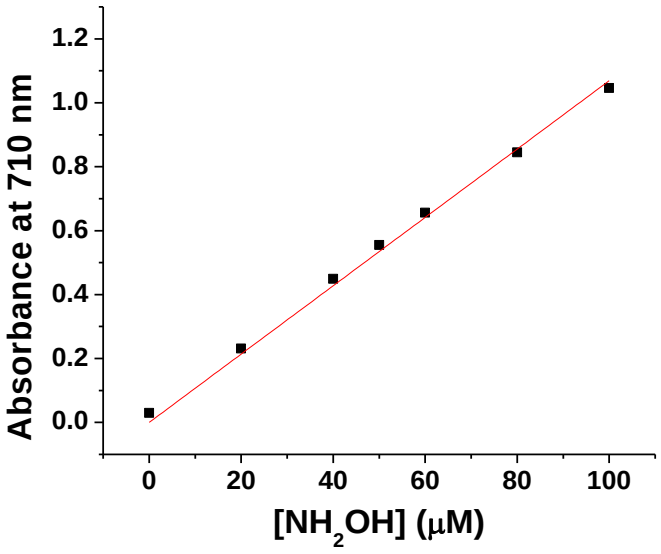

Figure 4: Calibration curve for the indooxine test showing a line of best fit for the plot of absorbance at 710 nm versus NH_2OH concentration. A linear fit with intercept forced through the origin gives a slope of $0.0107 \pm 0.0001\ \mu M^{-1}$.

Aqueous, anaerobic solutions of CHES buffer (5.0×10^{-3} M, pH 9.51) and CHES buffer (5.0×10^{-3} M, pH 9.51) containing $NaNO_2$ (2.96×10^{-4} M) were prepared. Cbl(I) was prepared (Section 2.3) and the concentration ($(1.28 \pm 0.05) \times 10^{-2}$ M) was determined by conversion to $(CN)_2Cbl^-$ (Section 2.5). The reaction of Cbl(I) ($200 \pm 7\ \mu M$) and $NaNO_2$ was carried out under anaerobic conditions for Cbl(I):NO_2^- ratios of 1:0.27 and 1:0.50, each in triplicate. After 1 hr reaction time, the indooxine test was performed on

each sample under aerobic conditions by combining the reaction product (1.00 mL) with 8-hydroxyquinoline solution (1.00 mL) and immediately adjusting the pH with Na_2CO_3 solution (1.00 mL). After 30 min at room temperature, the absorbance spectrum was collected (450 – 800 nm).

2.10 Indooxine Control Experiments

2.10.1 Testing for the Stability of Hydroxylamine in Anaerobic CHES Buffer

The stability of NH_2OH in neutral and alkaline solution was determined. An anaerobic solution of NH_2OH (10.00 mL, 2.93 x 10^{-3} M) was prepared and diluted (10.00 mL, 2.93 x 10^{-4} M) in the glove box. From this solution, an anaerobic NH_2OH solution (3.0 mL, 50 μM) was prepared in CHES buffer (5.0 x 10^{-3} M, pH 9.51) and an aerobic NH_2OH solution (3.0 mL, 50 μM) was prepared in water. After ~1 hr, the indooxine test was carried out on each sample, as described in Section 2.9, giving 48.1 μM NH_2OH for the sample in aerobic water and 52.2 μM for the sample in anaerobic pH 9.51 buffer.

2.10.2 Determining whether Cbl(II) Reacts with Hydroxylamine

A stock Cbl(II) solution was prepared according to the procedure described in Section 2.4 and the concentration (0.0172 M) was estimated by assuming the HOCbl·HCl reagent contained 12 % H_2O. An anaerobic NH_2OH stock solution was prepared in anaerobic water and diluted by a factor of 10 giving a concentration of 2.93 x 10^{-4} M. An aqueous, anaerobic Cbl(II) solution (3.0 mL, 50 μM) was prepared in water and an aqueous, anaerobic Cbl(II) (3.0 mL, 50 μM) solution containing NH_2OH (50 μM) was

prepared in CHES buffer (5.0×10^{-3} M, pH 9.51). UV-Vis spectra were collected for both solutions (250 – 800 nm) after 5, 15, and 25 min.

2.10.3 Determining whether Cbl(I) Reacts with Hydroxylamine

A stock Cbl(I) solution was prepared according to the procedure in Section 2.3 and the concentration (0.0130 M) was estimated by assuming the HOCbl·HCl reagent contained 12 % H_2O. An anaerobic NH_2OH stock solution was prepared in anaerobic water and diluted by a factor of 25 to give a concentration of 1.47×10^{-4} M. The spectrum of an aqueous, anaerobic Cbl(I) solution (3.0 mL, 50 μM) was compared with the spectrum of a solution of Cbl(I) (3.0 mL, 50 μM) and NH_2OH (50 μM) after 5, 15, and 25 min in CHES buffer (5.0×10^{-3} M, pH 9.51).

2.10.4 Determining whether Hydroxylamine Reacts with Nitrite or Acetone

NH_2OH (50 μM) was reacted separately with $NaNO_2$ (54 μM), acetone (6.3 μM, ~70x higher than the amount used in the indooxine test for NH_2OH, Section 2.9) or a solution containing $NaNO_2$ (54 μM) and acetone (6.3 μM) for 1 hr under anaerobic conditions in CHES buffer (5.0×10^{-3} M, pH 9.51, 3 mL reaction volume). An indooxine test was carried out on each sample in addition to a control NH_2OH solution (50 μM) of known concentration (Section 2.9). The absorbance of each solution at 710 nm was recorded and the NH_2OH concentration was determined using the calibration curve (Figure 4).

2.10.5 Determining the Hydroxylamine Content of the Cbl(I)/Nitrite Product Solution Spiked with Additional Hydroxylamine

In the glove box, Cbl(I) (200 μM, 0.600 mmol) was reacted with $NaNO_2$ (54 μM, 0.163 mmol, 1.0 mL reaction volume) in a 1:0.27 Cbl(I):NO_2^- ratio for 1 hr, in duplicate. The indooxine test (Section 2.9) was performed directly on one sample. An additional amount of NH_2OH (79.9 μM, 50.0 nmol, 2.0 mL reaction volume) was added to the second sample immediately prior to performing the indooxine test on that sample. An absorbance spectrum was collected (450 – 800 nm) and the absorbance at 710 nm was used to determine the NH_2OH concentration.

2.10.6 Determining if Nitrite Interferes with a Positive Indooxine Test

A solution of $NaNO_2$ was prepared in anaerobic CHES buffer (5.0×10^{-3} M, pH 9.51) An indooxine test was performed (Section 2.9) on the NO_2^- solution by combining 1.00 mL of the NO_2^- solution with the reagents for the indooxine test. An absorbance spectrum was collected (450 – 800 nm) and the absorbance at 710 nm was used to determine the NH_2OH concentration.

2.10.7 Determining whether the Presence of Cbl(II) has an Effect on Hydroxylamine Concentration Determined by the Indooxine Test Over Time

Cbl(II) was synthesized as described in Section 2.4 and the concentration (0.0154 M) was approximated by assuming the HOCbl·HCl contained 12 % H_2O. A stock NH_2OH solution (5.97×10^{-3} M) was prepared under anaerobic conditions and diluted by a factor of 10 with CHES buffer (pH 9.53, 5.0×10^{-3} M) to give 5.97×10^{-4} M NH_2OH. Anaerobic samples were prepared containing Cbl(II) (200 μM) and NH_2OH (50 μM) in

CHES buffer, and control samples were prepared containing NH_2OH (50 µM) only. The NH_2OH concentration was determined for the Cbl(II) + NH_2OH samples and control samples by the indooxine test (Section 2.9) after 0, 30, and 60 min under anaerobic conditions. All samples were prepared in duplicate.

2.10.8 Determining Whether Bubbling Air through Anaerobic Cbl(II) plus Hydroxylamimine Solutions Recovers NH_2OH

Cbl(II) was synthesized as described in Section 2.4 and the concentration (0.0154 M) was approximated by assuming the HOCbl·HCl contained 12 % H_2O. A stock NH_2OH solution (5.97×10^{-3} M) was prepared under anaerobic conditions and diluted by a factor of 10 with CHES buffer (pH 9.53, 5.0×10^{-3} M) to give 5.97×10^{-4} M NH_2OH. Anaerobic samples were prepared containing Cbl(II) (200 µM) and NH_2OH (50 µM) in CHES buffer, and control samples were prepared containing NH_2OH (50 µM) only. The NH_2OH concentration of the Cbl(II) + NO_2^- samples and control samples was determined by the indooxine test (Section 2.9) after 0, 3, and 10 min of bubbling air through the samples.

2.11 Determining whether Ammonia is a Product of the Reaction between Cbl(I) and Nitrite

A Nessler test for the presence of NH_3 was performed on a solution containing the reaction products of 200 µM Cbl(I) with 50 µM NO_2^- (0.050 M CHES buffer, pH 9.51) under aerobic conditions, in which the Cbl species was oxidized to HOCbl. Approximately 8 drops of the Nessler reagent were added to the product solution. A

positive result for NH_3 is indicated by a yellow or, at high concentrations, brown coloring in the reaction solution.[38] In this case, no brown or yellow coloring was observed above the pink color of the HOCbl species.

2.12 Kinetic Studies on the Reaction between Cbl(I) and Nitrite

All kinetic experiments for the reaction of Cbl(I) and NO_2^- were performed using at least ten times excess NO_2^- to ensure pseudo-first-order kinetics. A total ionic strength of 0.50 M was maintained for all experiments using Na_2HPO_4/NaH_2PO_4. Data at pH 10.80 were carried out in 0.050 M CAPS buffer using the Cary UV-Vis spectrophotometer and Schlenk cuvettes equipped with a cavity for the storage of the Cbl(I) reagent, allowing the Cbl(I) and NO_2^- reagents to be combined immediately before beginning data collection. The solutions were thermostated at 25.0 ˚C for at least 10 min before initiating the reaction. Data at pH < 10.80 were collected using the stopped-flow spectrophotometer in buffer (CHES, 0.050 M, pH 9.51; TAPS, 0.050 M, pH 8.51; phosphate, pH 7.40). Experiments performed at pH < 7.40 required that the buffer be mixed with a Cbl(I) solution in water as part of the stopped-flow procedure, since Cbl(I) is less stable in solution at lower pH. The Cbl(I) concentration was also elevated to 300 μM before mixing to provide additional stability. Buffers at pH 6.92 and 6.50 were prepared at twice the desired concentration and mixed with Cbl(I) within the stopped-flow itself. Data at pH 6.92 and 6.50 were carried out using 0.050 M buffers (BIS-TRIS and MES, respectively). Data at pH > 6.92 were collected and analyzed at 388 nm for

which the absorbance change for the reaction is largest. At pH 6.92 and 6.50, data was collected and analyzed at 500 nm to accommodate higher Cbl concentrations.

The source of the intercepts in the k_{obs} versus NO_2^- concentration plots at pH 6.92 and 6.50 (Figure 13(a,b), Section 3.5) was determined. Cbl(I) was diluted in anaerobic H_2O and was reacted with BIS-TRIS and MES buffers. Stopped-flow data at 500 nm was recorded for 60 sec.

III. RESULTS AND DISCUSSION

3.1 Attempts to Prepare Solid Cbl(I)

Cbl(I) is an unstable radical complex that requires a highly anaerobic environment for synthesis and storage. Others have termed it a supernucleophile that is known to react ~10^5 times faster than standard nucleophiles, such as thiols.[39,40] Moreover, slow spontaneous oxidation of Cbl(I) to Cbl(II) was observed in aqueous, anaerobic solution at room temperature. It was hypothesized that Cbl(I) may be more stable as a solid.

Three separate precipitations of Cbl(I) solution in chilled acetone were performed (Section 2.6). A fraction of the precipitated Cbl(I) was immediately re-dissolved in anaerobic water and the UV-Vis spectrum recorded. The results from the most successful trial are shown in Figure 5. The results of this experiment were not reproduced well by the other two trials, which yielded more significant oxidation of Cbl(I) to Cbl(II) immediately after precipitation. The most successful precipitation procedure resulted in ~10% oxidation of Cbl(I) to Cbl(II) immediately after precipitation. The precipitated Cbl(I) sample was re-dissolved in water after 11 days of storage in the freezer of the glove box (-24 °C), and analyzed by UV-Vis spectrophotometry. The spectrum indicated complete conversion to Cbl(II) after 11 days of storage. It was therefore determined that precipitation by addition to chilled acetone does not achieve pure solid Cbl(I).

Alternatively, attempts were made to synthesize solid Cbl(I) by evaporation of the solvent of a Cbl(I) solution under vacuum. This method, however, requires a lengthy

period in which Cbl(I) is in solution at room temperature. The obtained solid was re-dissolved in H_2O, a UV-Vis spectrum obtained, and found to be ~70% oxidized to Cbl(II). Thus, both methods failed to produce pure Cbl(I) in the solid state. Consequentially, all of the subsequent experiments were carried out using freshly prepared Cbl(I) in solution as the Cbl(I) reagent.

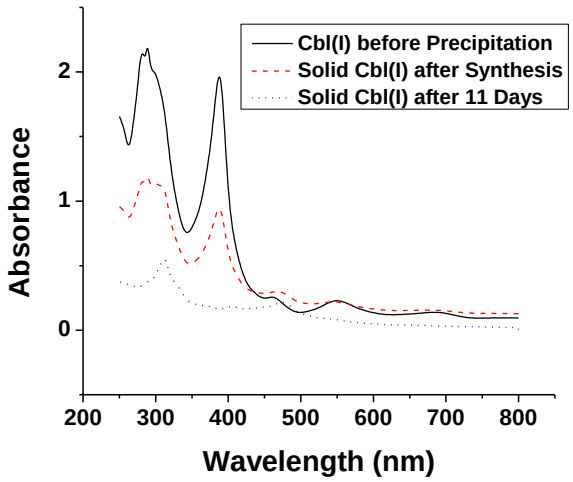

Figure 5: UV-Vis spectra of Cbl(I) (λ_{max} 280, 288, 386, 455, 545, 680 nm[35]) before precipitation (solid trace) and after precipitation and resuspension in solution. Immediately following precipitation, Cbl(I) was partially (~10%) oxidized to Cbl(II) (λ_{max} 267, 285, 315, 467 nm[35]) (dashed trace). 11 days after precipitation, near complete oxidation to Cbl(II) (70 %) was observed (dotted trace). Large differences in absorbance are primarily due to differences in concentration of the samples.

3.2 Identification of Cbl(II) as the Cbl Product of the Reaction of Cbl(I) with Nitrite

The Cbl product of the reaction of Cbl(I) with NO_2^- was identified by UV-Vis spectrophotometry (Section 2.7). UV-Vis spectral data as a function of time were collected for the reaction of Cbl(I) (50 μM) with NO_2^- (9.1 mM), in phosphate buffer

(0.050 M, pH 12.00), Figure 6(a). The initial and final spectra correspond to that of Cbl(I), and Cbl(II) respectively, Figure 6(b). From Figure 6(a) it can be seen that the reaction exhibits clean isosbestic points at 307, 346, 417 and 543 nm in agreement with literature values for the conversion of Cbl(I) to Cbl(II),[41] indicating a direct and clean conversion of Cbl(I) to Cbl(II) for the rate-determining step of the reaction.

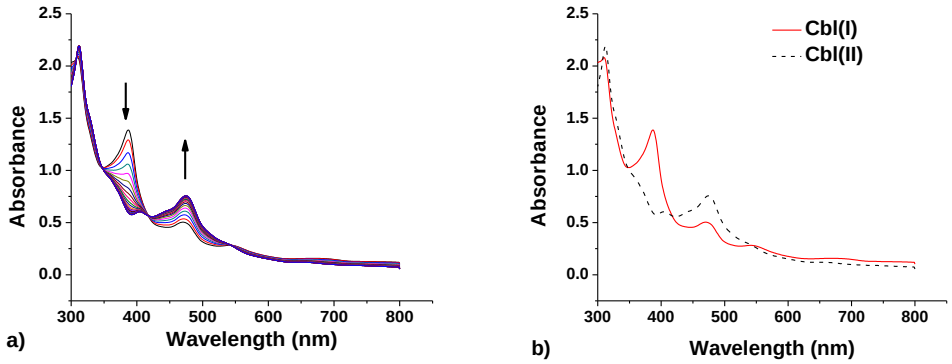

Figure 6: (a) UV-Vis spectra as a function of time for the reaction of Cbl(I) (λ_{max} 280, 288, 386, 455, 545, and 680 nm,[35] 50 μM) with NO_2^- (9.1 mM) in 0.050 M phosphate buffer at pH 12.00, 25.0 ˚C. Spectra were recorded every 2.5 min for 40 min. (b) Initial and final spectra for the reaction shown in (a). The final spectrum corresponds to that of Cbl(II) (λ_{max} 267, 285, 315, 467 nm[35]).

3.3 Determination of the Stoichiometry of the Reaction of Cbl(I) with Nitrite

UV-Vis spectra of the product solution obtained upon equilibrating Cbl(I) (200 μM) with 0 – 0.50 mole equiv. NO_2^- under anaerobic conditions were recorded for pH 9.51 (5.0 x 10^{-3} M CHES, 25.0 °C). The Cbl(I) concentration was elevated for this experiment to enhance its stability in buffered solution. The minimum time for the reaction to proceed to completion was found to be ~30 min, so each solution was allowed

to react under anaerobic conditions for at least this amount of time. The absorbance at 700 nm (Figure 7(a)) and 500 nm (Figure 7(b)) for each reaction was plotted against the mole equiv. of NO_2^- added. These wavelengths were found to be convenient for analysis because the absorbance of the Cbl species is within the detectable range for the instrument at these wavelengths (Abs < 2). From these plots, it is clear that the reaction is complete after the addition of ~0.25 mole equiv. of NO_2^-. Tables 1 and 2 summarize the experimental data obtained at 700 and 500 nm, respectively. The mean value of the equiv. of NO_2^- required is 0.24 ± 0.02. This suggests a 4:1 Cbl(I):NO_2^- mole ratio.

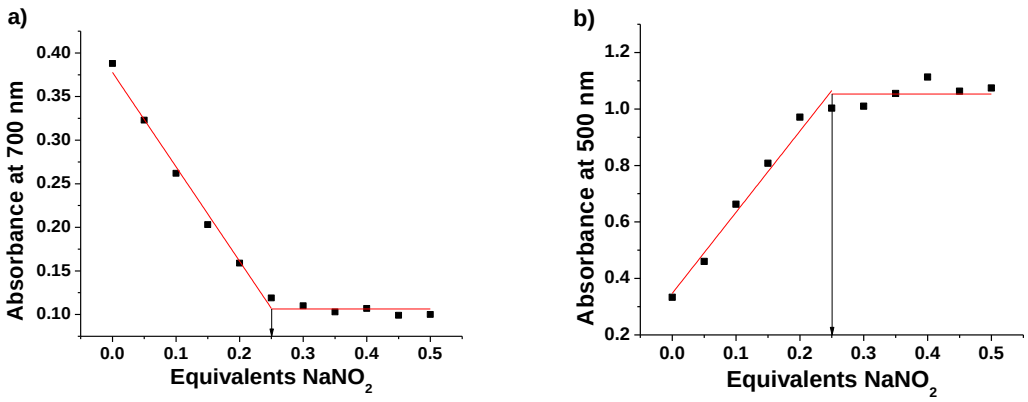

Figure 7: Plot of absorbance at (a) 700 nm or (b) 500 nm versus mole equiv. of $NaNO_2$ for equilibrated solutions of Cbl(I) (200 ± 9 μM) with NO_2^- (5.0×10^{-3} M, CHES buffer, pH 9.51, 25.0 °C).

The stoichiometry experiment was repeated at pH 9.53 using a slightly modified procedure for determination of the Cbl(I) concentration (Section 2.8). Once again, the number of mole equiv. of NO_2^- added was varied and the absorbance at 700 nm (Figure 8(a)) and 500 nm (Figure 8(b)) for each reaction was plotted against the number of NO_2^- equiv. added. Tables 3 and 4 summarize the data, which gives a mean value of

Table 1: Determination of the stoichiometry of the reaction between Cbl(I) and NO_2^- at pH 9.51 (5.0×10^{-3} M CHES buffer). Absorbances were measured at 700 nm.

[a]Fraction Cbl(I) Reacted = $(Abs_{Cbl(I)} - Abs_{obs}) / (Abs_{Cbl(I)} - Abs_{Cbl(II)})$

[b]Mole Equiv. NO_2^- Required = $([NO_2^-]_i / [Cbl(I)]_i)$ / Fraction Cbl(I) Reacted

$10^4[Cbl(I)]_i$ (M)	$10^5[NO_2^-]_i$ (M)	$[NO_2^-]_i / [Cbl(I)]_i$	$Abs_{Cbl(I)}$	$Abs_{Cbl(II)}$	Abs_{obs}	Fraction Cbl(I) Reacted[a]	Mole Equiv. NO_2^- Required[b]
2.00	1.00	0.050	0.388	0.104	0.323	0.229	0.22
2.00	2.00	0.10	0.388	0.104	0.262	0.443	0.23
2.00	3.00	0.15	0.388	0.104	0.203	0.651	0.23
2.00	4.00	0.20	0.388	0.104	0.159	0.806	0.25
2.00	5.00	0.25	0.388	0.104	0.119	0.947	0.26
2.00	6.00	0.30	0.388	0.104	0.110	-	-
2.00	7.00	0.35	0.388	0.104	0.103	-	-
2.00	8.00	0.40	0.388	0.104	0.107	-	-
2.00	9.00	0.45	0.388	0.104	0.099	-	-
2.00	10.0	0.50	0.388	0.104	0.100	-	-

Table 2: Determination of the stoichiometry of the reaction between Cbl(I) and NO_2^- at pH 9.51 (5.0×10^{-3} M CHES buffer). Absorbances were measured at 500 nm.

[a]Fraction Cbl(I) Reacted = $(Abs_{Cbl(I)} - Abs_{obs}) / (Abs_{Cbl(I)} - Abs_{Cbl(II)})$

[b]Mole Equiv. NO_2^- Required = $([NO_2^-]_i / [Cbl(I)]_i)$ / Fraction Cbl(I) Reacted

$10^4[Cbl(I)]_i$ (M)	$10^5[NO_2^-]_i$ (M)	$[NO_2^-]_i / [Cbl(I)]_i$	$Abs_{Cbl(I)}$	$Abs_{Cbl(II)}$	Abs_{obs}	Fraction Cbl(I) Reacted[a]	Mole Equiv. NO_2^- Required[b]
2.00	1.00	0.050	0.334	1.06	0.46	0.173	0.29
2.00	2.00	0.10	0.334	1.06	0.663	0.452	0.22
2.00	3.00	0.15	0.334	1.06	0.808	0.650	0.23
2.00	4.00	0.20	0.334	1.06	0.971	0.874	0.23
2.00	5.00	0.25	0.334	1.06	1.00	0.918	0.27
2.00	6.00	0.30	0.334	1.06	1.01	-	-
2.00	7.00	0.35	0.334	1.06	1.06	-	-
2.00	8.00	0.40	0.334	1.06	1.11	-	-
2.00	9.00	0.45	0.334	1.06	1.06	-	-
2.00	10.0	0.50	0.334	1.06	1.07	-	-

0.26 ± 0.02 mole equiv. NO_2^-. This value is in excellent agreement with that obtained from the earlier experiment. Combining the results of both experiments gives a NO_2^-:Cbl(I) stoichiometry of (0.25 ± 0.02):1.

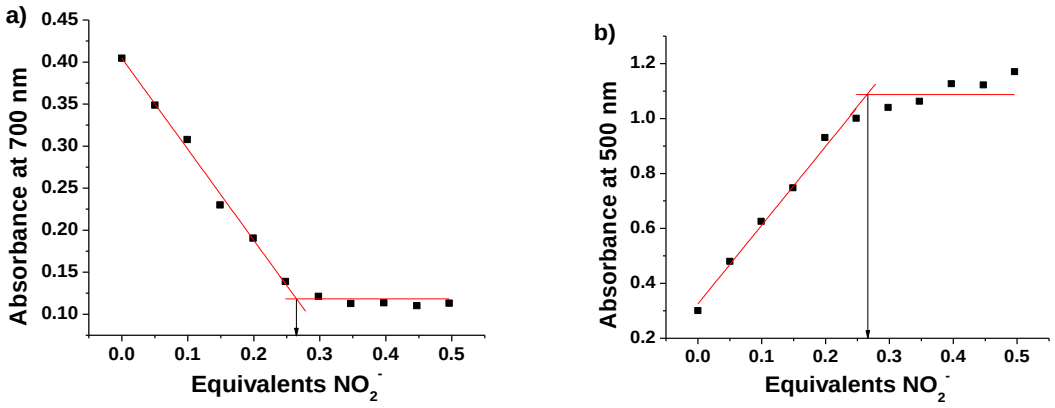

Figure 8: Plot of absorbance at (a) 700 nm or (b) 500 nm versus mole equiv. $NaNO_2$ for equilibrated solutions of Cbl(I) (200 ± 8 μM) with NO_2^- (5.0 x 10^{-3} M CHES buffer, pH 9.53, 25.0 °C).

The stoichiometry for the reaction of Cbl(I) and NO_2^- was also determined at pH 7.40 (5.0 x 10^{-3} M phosphate buffer). The minimum time for the reaction to equilibrate was found to be < 1.5 min (the time required to remove the sample from the glove box). As before, the absorbance at 700 nm (Figure 9 (a)) and 500 nm (Figure 9(b)) for each reaction was plotted against the mole equiv. of NO_2^- added. Again, these plots show that the reaction is complete after the addition of ~0.25 mole equiv. of NO_2^-. The experimental data for 700 and 500 nm is summarized in Tables 5 and 6, respectively. The mean value of the equiv. of NO_2^- required is 0.28 ± 0.03 equiv NO_2^-. The expected number of equivalents (0.25 equiv.) is contained within the statistical error of the result.

Table 3: Determination of the stoichiometry of the reaction between Cbl(I) and NO_2^- at pH 9.53 (5.0×10^{-3} M CHES buffer). Absorbances were measured at 700 nm.

[a]Fraction Cbl(I) Reacted = $(Abs_{Cbl(I)} - Abs_{obs}) / (Abs_{Cbl(I)} - Abs_{Cbl(II)})$

[b]Mole Equiv. NO_2^- Required = $([NO_2^-]_i / [Cbl(I)]_i)$ / Fraction Cbl(I) Reacted

$10^4[Cbl(I)]_i$ (M)	$10^5[NO_2^-]_i$ (M)	$[NO_2^-]_i / [Cbl(I)]_i$	$Abs_{Cbl(I)}$	$Abs_{Cbl(II)}$	Abs_{obs}	Fraction Cbl(I) Reacted[a]	Mole Equiv. NO_2^- Required[b]
2.01	1.00	0.050	0.405	0.114	0.349	0.192	0.26
2.01	2.00	0.10	0.405	0.114	0.308	0.333	0.30
2.01	3.00	0.15	0.405	0.114	0.230	0.601	0.25
2.01	4.00	0.20	0.405	0.114	0.191	0.737	0.27
2.01	5.00	0.25	0.405	0.114	0.139	0.914	0.27
2.01	6.00	0.30	0.405	0.114	0.121	-	-
2.01	7.00	0.35	0.405	0.114	0.113	-	-
2.01	8.00	0.40	0.405	0.114	0.114	-	-
2.01	9.00	0.45	0.405	0.114	0.110	-	-
2.01	10.0	0.50	0.405	0.114	0.113	-	-

Table 4: Determination of the stoichiometry of the reaction between Cbl(I) and NO_2^- at pH 9.53 (5.0×10^{-3} M CHES buffer). Absorbances were measured at 500 nm.

[a]Fraction Cbl(I) Reacted = $(Abs_{Cbl(I)} - Abs_{obs}) / (Abs_{Cbl(I)} - Abs_{Cbl(II)})$

[b]Mole Equiv. NO_2^- Required = $([NO_2^-]_i / [Cbl(I)]_i)$ / Fraction Cbl(I) Reacted

$10^4[Cbl(I)]_i$ (M)	$10^5[NO_2^-]_i$ (M)	$[NO_2^-]_i / [Cbl(I)]_i$	$Abs_{Cbl(I)}$	$Abs_{Cbl(II)}$	Abs_{obs}	Fraction Cbl(I) Reacted[a]	Mole Equiv. NO_2^- Required[b]
2.01	1.00	0.050	0.300	1.104	0.4801	0.223	0.22
2.01	2.00	0.10	0.300	1.104	0.6261	0.405	0.25
2.01	3.00	0.15	0.300	1.104	0.748	0.557	0.27
2.01	4.00	0.20	0.300	1.104	0.9308	0.784	0.26
2.01	5.00	0.25	0.300	1.104	1.001	0.871	0.29
2.01	6.00	0.30	0.300	1.104	1.0405	-	-
2.01	7.00	0.35	0.300	1.104	1.0628	-	-
2.01	8.00	0.40	0.300	1.104	1.1265	-	-
2.01	9.00	0.45	0.300	1.104	1.1221	-	-
2.01	10.0	0.50	0.300	1.104	1.1704	-	-

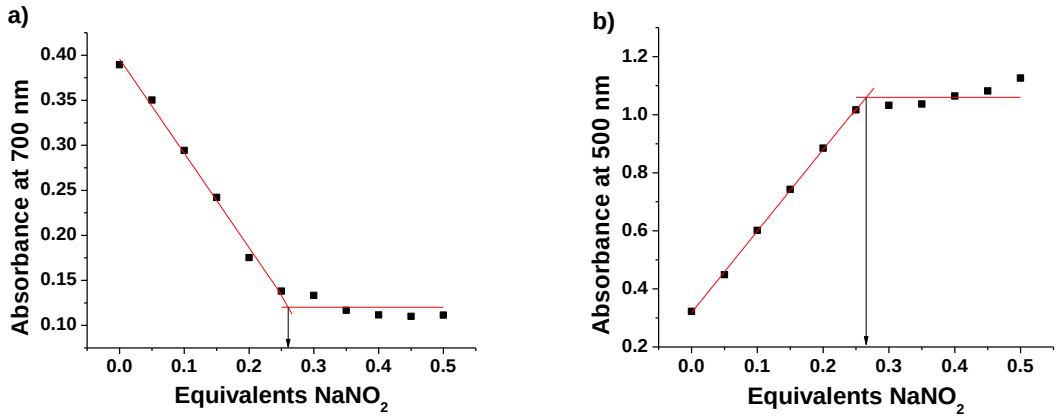

Figure 9: Plot of absorbance at (a) 700 nm or (b) 500 nm versus mole equiv. $NaNO_2$ for equilibrated solutions of Cbl(I) (200 ± 3 μM) with NO_2^- (5.0 x 10^{-3} M phosphate buffer, pH 7.40, 25.0 °C)

Table 5: Determination of the stoichiometry of the reaction between Cbl(I) and NO_2^- at pH 7.40 (5.0 x 10^{-3} M phosphate buffer). Absorbances were measured at 700 nm.

[a]Fraction Cbl(I) Reacted = $(Abs_{Cbl(I)} - Abs_{obs}) / (Abs_{Cbl(I)} - Abs_{Cbl(II)})$

[b]Mole Equiv. NO_2^- Required = $([NO_2^-]_i / [Cbl(I)]_i)$ / Fraction Cbl(I) Reacted

$10^4[Cbl(I)]_i$ (M)	$10^5[NO_2^-]_i$ (M)	$[NO_2^-]_i / [Cbl(I)]_i$	$Abs_{Cbl(I)}$	$Abs_{Cbl(II)}$	Abs_{obs}	Fraction Cbl(I) Reacted[a]	Mole Equiv. NO_2^- Required[b]
2.00	1.00	0.050	0.389	0.120	0.350	0.146	0.34
2.00	2.00	0.10	0.389	0.120	0.294	0.354	0.28
2.00	3.00	0.15	0.389	0.120	0.242	0.547	0.27
2.00	4.00	0.20	0.389	0.120	0.175	0.795	0.25
2.00	5.00	0.25	0.389	0.120	0.138	0.93	0.27
2.00	6.00	0.30	0.389	0.120	0.133	-	-
2.00	7.00	0.35	0.389	0.120	0.117	-	-
2.00	8.00	0.40	0.389	0.120	0.112	-	-
2.00	9.00	0.45	0.389	0.120	0.110	-	-
2.00	10.0	0.50	0.389	0.120	0.111	-	-

Table 6: Determination of the stoichiometry of the reaction between Cbl(I) and NO_2^- at pH 7.40 (5.0 x 10^{-3} M phosphate buffer). Absorbances were measured at 500 nm.

[a]Fraction Cbl(I) Reacted = $(Abs_{Cbl(I)} - Abs_{obs}) / (Abs_{Cbl(I)} - Abs_{Cbl(II)})$

[b]Mole Equiv. NO_2^- Required = $([NO_2^-]_i/[Cbl(I)]_i)$ / Fraction Cbl(I) Reacted

$10^4[Cbl(I)]_i$ (M)	$10^5[NO_2^-]_i$ (M)	$[NO_2^-]_i/[Cbl(I)]_i$	$Abs_{Cbl(I)}$	$Abs_{Cbl(II)}$	Abs_{obs}	Fraction Cbl(I) Reacted[a]	Mole Equiv. NO_2^- Required[b]
2.00	1.00	0.050	0.322	1.06	0.449	0.172	0.29
2.00	2.00	0.10	0.322	1.06	0.601	0.378	0.26
2.00	3.00	0.15	0.322	1.06	0.743	0.570	0.26
2.00	4.00	0.20	0.322	1.06	0.885	0.763	0.26
2.00	5.00	0.25	0.322	1.06	1.02	0.94	0.27
2.00	6.00	0.30	0.322	1.06	1.03	-	-
2.00	7.00	0.35	0.322	1.06	1.04	-	-
2.00	8.00	0.40	0.322	1.06	1.06	-	-
2.00	9.00	0.45	0.322	1.06	1.08	-	-
2.00	10.0	0.50	0.322	1.06	1.13	-	-

The stoichiometry experiment at pH 7.40 (5.0 x 10^{-3} M phosphate buffer) was repeated to verify the result. The absorbance at 700 nm (Figure 10(a)) and 500 nm

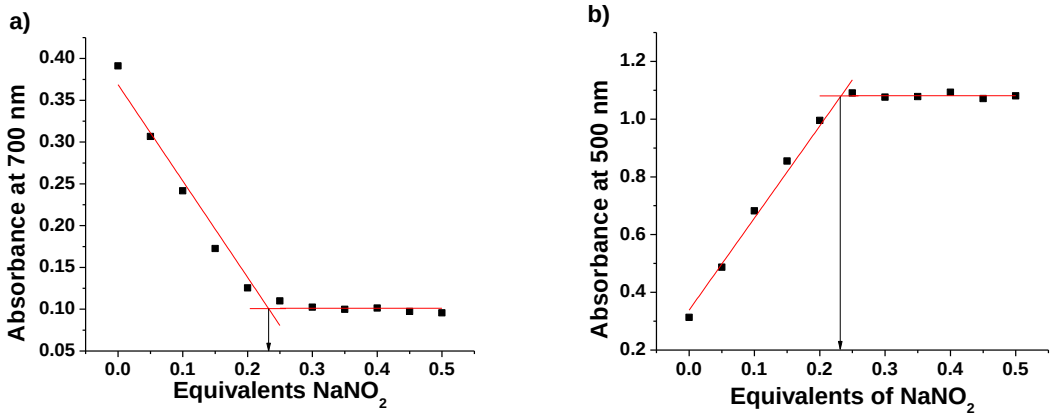

Figure 10: Plot of absorbance at (a) 700 nm or (b) 500 nm versus mole equiv. $NaNO_2$ for equilibrated solutions of Cbl(I) (200 ± 6 μM) with NO_2^- (5.0 x 10^{-3} M phosphate buffer, pH 7.40, 25.0 °C).

(Figure 10(b)) for each reaction was plotted against the mole equiv. of NO_2^- added. The experimental data for 700 and 500 nm is summarized in Tables 7 and 8, respectively. The mean value of the equiv. of NO_2^- required was determined to be 0.22 ± 0.02 equiv NO_2^-. This result suggests the possibility of a $5e^-$ process; however this would result in reduction of nitrogen to the -2 oxidation state. This is unlikely, which suggests that the reaction stoichoimetry is 4:1 Cbl(I):NO_2^- at pH 7.40. Combining the results of both experiments at pH 7.40 gives a NO_2^-:Cbl(I) stoichiometry of (0.25 ± 0.04):1. The reaction stoichiometry was, therefore, found to be 0.25: 1 NO_2^-:Cbl(I) for both pH 9.51 and pH 7.40.

Table 7: Determination of the stoichiometry of the reaction between Cbl(I) and NO_2^- at pH 7.40 (5.0×10^{-3} M phosphate buffer). Absorbances were measured at 700 nm.
[a]Fraction Cbl(I) Reacted = $(Abs_{Cbl(I)} - Abs_{obs}) / (Abs_{Cbl(I)} - Abs_{Cbl(II)})$
[b]Mole Equiv. NO_2^- Required = $([NO_2^-]_i / [Cbl(I)]_i)$ / Fraction Cbl(I) Reacted

$10^4[Cbl(I)]_i$ (M)	$10^5[NO_2^-]_i$ (M)	$[NO_2^-]_i / [Cbl(I)]_i$	$Abs_{Cbl(I)}$	$Abs_{Cbl(II)}$	Abs_{obs}	Fraction Cbl(I) Reacted[a]	Mole Equiv. NO_2^- Required[b]
2.00	1.00	0.050	0.391	0.101	0.307	0.291	0.17
2.00	2.00	0.10	0.391	0.101	0.242	0.515	0.19
2.00	3.00	0.15	0.391	0.101	0.173	0.753	0.20
2.00	4.00	0.20	0.391	0.101	0.126	0.916	0.22
2.00	5.00	0.25	0.391	0.101	0.110	0.97	0.26
2.00	6.00	0.30	0.391	0.101	0.102	-	-
2.00	7.00	0.35	0.391	0.101	0.100	-	-
2.00	8.00	0.40	0.391	0.101	0.101	-	-
2.00	9.00	0.45	0.391	0.101	0.0974	-	-
2.00	10.0	0.50	0.391	0.101	0.0956	-	-

Table 8: Determination of the stoichiometry of the reaction between Cbl(I) and NO_2^- at pH 7.40 (5.0×10^{-3} M phosphate buffer). Absorbances were measured at 500 nm.
[a]Fraction Cbl(I) Reacted = $(Abs_{Cbl(I)} - Abs_{obs}) / (Abs_{Cbl(I)} - Abs_{Cbl(II)})$
[b]Mole Equiv. NO_2^- Required = $([NO_2^-]_i / [Cbl(I)]_i)$ / Fraction Cbl(I) Reacted

$10^4[Cbl(I)]_i$ (M)	$10^5[NO_2^-]_i$ (M)	$[NO_2^-]_i / [Cbl(I)]_i$	$Abs_{Cbl(I)}$	$Abs_{Cbl(II)}$	Abs_{obs}	Fraction Cbl(I) Reacted[a]	Mole Equiv. NO_2^- Required[b]
2.00	1.00	0.050	0.313	1.08	0.487	0.226	0.22
2.00	2.00	0.10	0.313	1.08	0.682	0.480	0.21
2.00	3.00	0.15	0.313	1.08	0.855	0.705	0.21
2.00	4.00	0.20	0.313	1.08	0.995	0.888	0.23
2.00	5.00	0.25	0.313	1.08	1.09	1.01	0.25
2.00	6.00	0.30	0.313	1.08	1.08	-	-
2.00	7.00	0.35	0.313	1.08	1.08	-	-
2.00	8.00	0.40	0.313	1.08	1.09	-	-
2.00	9.00	0.45	0.313	1.08	1.07	-	-
2.00	10.0	0.50	0.313	1.08	1.08	-	-

3.4 Determining the Amount of Hydroxylamine Product Formed in the Reaction of Cbl(I) with Nitrite

A 0.25:1 NO_2^-:Cbl(I) reaction stoichiometry suggests that the non-Cbl reaction product is NH_2OH. Whether the reactive species is NO_2^- or HNO_2 will be considered later. The balanced equation for the reaction is shown in equation (1).

$$(4)5H^+ + 4Cbl(I)^- + (H)NO_2 \longrightarrow 4Cbl(II) + NH_2OH + H_2O \quad (1)$$

An indooxine test for the presence of NH_2OH was carried out as described in Section 2.9. A calibration curve (absorbance at 710 nm versus NH_2OH concentration) was generated and is shown in Figure 4, Section 2.9. Cbl(I) and NO_2^- were combined in 1:0.27 (near

stoichiometric) and 1:0.50 (excess NO_2^-) mole ratios and the indooxine test was performed on these solutions. Only the indooxine product absorbs in the 650 – 750 nm region (λ_{max} 710 nm[37]) and the NH_2OH concentration was determined by use of the calibration curve in Figure 4, Section 2.9. Table 9 summarizes the results. The average NH_2OH concentration in the product solution was found to be 21 ± 2 μM. Given that 200 μM Cbl(I) was reacted with sufficient NO_2^- for the reaction to proceed to completion according to the results of the stoichiometry experiment, 50.0 μM NH_2OH should theoretically be produced for both 1:0.27 and 1:0.50 Cbl(I):NO_2^- ratios. However, only ~40 % of the NH_2OH product (21 ± 2 μM) was obtained using the indooxine test to quantify the amount of product formed for both reactant ratios.

The low recovery of the NH_2OH species by the indooxine test was investigated. A series of control experiments to determine what was responsible for the reduced yield of NO_2^- were undertaken. First, the stability of NH_2OH in anaerobic CHES buffer (pH 9.51)

Table 9: Detection of NH_2OH by the indooxine test, confirming NH_2OH as a reaction product in the reaction of Cbl(I) (200 ± 7 μM) with NO_2^- (0.27 and 0.50 mole equiv.) in CHES buffer (5.0 x 10^{-3} M, pH 9.51). The NH_2OH concentration was calculated based on the calibration curve in Figure 4, Section 2.9. The average concentration was 21 ± 2 μM.

Equivalents of NO_2^-	**Absorbance at 710 nm**	**Concentration of NH_2OH (μM)**
0.27	0.210	19.6
0.27	0.206	19.3
0.27	0.206	19.3
0.5	0.220	20.6
0.5	0.228	21.3
0.5	0.258	24.1

was determined (Section 2.10.1). NH_2OH (50 μM) was incubated in anaerobic CHES buffer and aerobic water for ~1 hr and an indooxine test was used to quantify the amount of NH_2OH in each solution. The determined NH_2OH concentrations were 48.1 μM for the sample in aerobic water and 52.2 μM for the sample in anaerobic pH 9.51 buffer. Hence the alkaline pH, the presence or absence of air, and the presence of the CHES buffer in the NH_2OH sample have no effect within experimental error on the NH_2OH concentration determined using the indooxine method; that is, NH_2OH is stable in solution under these conditions.

Another possibility is that some of the NH_2OH product was oxidized to N_2. The reduction potentials of N_2/NH_2OH, Cbl(III)/Cbl(II), and Cbl(II)/Cbl(I) are -3.04 V (pH 14),[42] 0.200 V, and -0.600 V[20] versus SHE, respectively. The stability of Cbl(II) and Cbl(I) in solution with NH_2OH was determined by observing the spectrum of Cbl(II) (50 μM) and Cbl(I) (50 μM) in solution with NH_2OH (50 μM) by UV-Vis spectrophotometry (Sections 2.10.2 and 2.10.3). It was found that the spectra of Cbl(II) and Cbl(I) do not change over 25 min when NH_2OH is added under anaerobic conditions; hence neither Cbl(II) nor Cbl(I) are reduced by NH_2OH under our experimental conditions.

Others have reported that NH_2OH reacts with NO_2^-, albeit under strongly acidic conditions.[43] Whether this reaction occurs under our experimental conditions was therefore also investigated (Section 2.10.4). The potential of NH_2OH to react with the small amount of acetone originating from the synthesis of Cbl(I) (Section 2.3) in the product mixture was also investigated (Section 2.10.4). The results of the indooxine test for NH_2OH concentration showed that the NH_2OH does not decompose or react further

under the experimental conditions used in the presence of $NaNO_2$ (54 μM) or acetone (6.3 μM), or both $NaNO_2$ and acetone.

To ensure that the indooxine test was reliable for the experimental conditions used, the indooxine test was performed on a Cbl(I) + NO_2^- product sample which was spiked with an additional 50.0 nmol NH_2OH (Section 2.10.5). Using the calibration curve (Figure 4, Section 2.9), it was determined that the unspiked sample contained 10.9 μM (10.9 nmol) NH_2OH and the spiked sample contained 29.4 μM (58.8 nmol) NH_2OH. The spiked sample gave the expected increase in NH_2OH content.

Excess NO_2^- present in solution may cause interference with the indooxine test under certain conditions.[37] The indooxine test for the NH_2OH product of the reaction between Cbl(I) and NO_2^- was performed using no more than 50 μM excess NO_2^-. Therefore, the indooxine test was performed on a sample containing 50 μM NO_2^- under the conditions used for the quantification of NH_2OH produced by the Cbl(I) + NO_2^- reaction (Section 2.10.6). It was found that NO_2^- does not interfere with the indooxine test at this concentration.

A control experiment was also performed to test the effect of the presence of Cbl(II) (200 μM) on NH_2OH (50 μM) for 0, 30, and 60 min under anaerobic conditions (Section 2.10.7). The indooxine test showed that ~30 % of the original NH_2OH is absent from the samples containing Cbl(II) regardless of how long the solution was allowed to react (0, 30, or 60 min), while at least 95 % of the NH_2OH was recovered in the solutions that did not contain Cbl(II) (Table 10). Additionally, since the indooxine reaction requires aerobic conditions, a control experiment was done to determine the effect of bubbling air

through the Cbl(I) + NO_2^- product solution prior to performing the indooxine test (Section 2.10.8). It was found that bubbling for 3 min recovered ~80 % of the original NH_2OH concentration, but further bubbling for 10 min was unsuccessful at recovering the remaining NH_2OH (Table 11). Importantly, transition metal-catalyzed disproportionation of NH_2OH has been reported by others.[44,45] It is likely that aqueous reduced products of the disproportionated NH_2OH are re-oxidized to NH_2OH in the presence of oxygen, but the gaseous and oxidized products are not retrieved. Under anaerobic conditions in the presence of transition metals, NH_2OH disproportionates to give N_2, N_2O, and NO^+.[44]

Finally, a test was performed to determine whether NH_3 is a product of the reaction of Cbl(I) and NO_2^- (Section 2.11). Cbl(I) (200 μM) was reacted with NO_2^- (50 μM) under anaerobic conditions (0.050 M CHES buffer, pH 9.51). Nessler reagent was added (~8 drops) under aerobic conditions to the product solution. A color change to yellow or brown is indicative of the presence of NH_3. Since no color change was observed, NH_3 is not a product of the reaction of Cbl(I) and NO_2^-.

To summarize, the results of the stoichiometry experiment suggest that the stoichiometry of the reaction between Cbl(I) and NO_2^- is 4:1 Cbl(I):NO_2^-. Cbl(II) was shown to be the Cbl product by UV-Vis spectrophotometry. The expected non-Cbl product is NH_2OH, and the balanced equation is given by equation (1). The indooxine test for the presence of NH_2OH was positive, albeit non-quantitative, in agreement with the elucidated reaction stoichiometry. It is likely that some of the NH_2OH disproportionates; hence the lower yield of NH_2OH.

Table 10: Absorbance obtained at 710 nm for solutions of NH_2OH (50 μM) in the absence and presence of Cbl(II) (200 μM). Solutions were left to react under anaerobic conditions for 0, 30, and 60 min prior to determining the NH_2OH concentration using the indooxine test. [a]Determined from the calibration curve shown in Figure 4, Section 2.9.

Contents	Replicate	Time under anaerobic conditions (min)	Absorbance at 710 nm	Concentration of NH_2OH (μM)[a]
NH_2OH	1	0	0.499	46.6
NH_2OH	2	0	0.538	50.3
NH_2OH + Cbl(II)	1	0	0.357	33.4
NH_2OH + Cbl(II)	2	0	0.365	34.1
NH_2OH	1	30	0.502	46.9
NH_2OH	2	30	0.517	48.3
NH_2OH + Cbl(II)	1	30	0.336	31.4
NH_2OH + Cbl(II)	2	30	0.338	31.6
NH_2OH	1	60	0.513	47.9
NH_2OH	2	60	0.518	48.4
NH_2OH + Cbl(II)	1	60	0.346	32.3
NH_2OH + Cbl(II)	2	60	0.346	32.3

Table 11: Absorbance obtained at 710 nm for solutions of NH_2OH (50 μM) in the absence and presence of Cbl(II) (200 μM). Air was bubbled through the solutions for 0, 3, or 10 min prior to determining the NH_2OH concentration using the indooxine test. [a]Determined from the calibration curve shown in Figure 4, Section 2.9.

Contents	Replicate	Air bubbling time (min)	Absorbance at 710 nm	Concentration of NH_2OH (μM)[a]
NH_2OH	1	0	0.499	46.6
NH_2OH	2	0	0.538	50.3
NH_2OH + Cbl(II)	1	0	0.357	33.4
NH_2OH + Cbl(II)	2	0	0.365	34.1
NH_2OH	1	3	0.535	50.0
NH_2OH	2	3	0.548	51.2
NH_2OH + Cbl(II)	1	3	0.439	41.0
NH_2OH + Cbl(II)	2	3	0.434	40.6
NH_2OH	1	10	0.532	49.7
NH_2OH	2	10	0.525	49.7
NH_2OH + Cbl(II)	1	10	0.436	40.7
NH_2OH + Cbl(II)	2	10	0.439	41.0

3.5 Kinetic Studies on the reaction of Cbl(I) with Nitrite

The kinetics of the reaction of Cbl(I) with NO_2^- were studied at pH 6.50 (0.050 M MES), 6.92 (0.050 M BIS-TRIS), 7.40 (phosphate), 8.51 (0.050 M TAPS), 9.51 (0.050 M CHES), and 10.80 (0.050 M CAPS) at 25 °C. Data were collected under pseudo-first-order conditions in which the NO_2^- concentration was at least ten times greater than the Cbl(I) concentration. This method allows for direct determination of the reaction order for each reactant. Figure 11(a) gives a typical plot of absorbance versus time for the reaction of Cbl(I) (50 μM) with NO_2^- (5.0 mM). The first-order integrated rate equation

$$A_{obs} = A_f + (A_0 - A_f)e^{-k_{obs}\, t} \qquad (2)$$

was used to fit the data, where A_{obs} is observed absorbance, A_f is final absorbance, A_0 is initial absorbance, k_{obs} is the observed rate constant, and t is time. The data fit well to equation (2), suggesting that the reaction is first-order with respect to the Cbl(I) concentration. Figure 11(b) gives a plot of absorbance versus time for the Cbl(I) solution in the absence of NO_2^- at pH 10.80. Cbl(I) is slowly oxidized to Cbl(II); however, this reaction is significantly slower than the reaction of interest at pH 10.80. The change in absorbance (ΔA) for the complete reaction between Cbl(I) and NO_2^- (Figure 11(a)) was 0.45 at 388 nm. Oxidation of Cbl(I) in buffer over this same period of time (Figure 11(b)) gave a ΔA of 0.02 at 388 nm, which amounts to 5 % of the total absorbance change. Thus, at pH 10.80, the oxidation of Cbl(I) in buffer is negligible with respect to the rate of the Cbl(I) + NO_2^- reaction. The rate of oxidation of Cbl(I) to Cbl(II) in buffer alone can in fact be determined from the intercept of the k_{obs} versus NO_2^- plots.

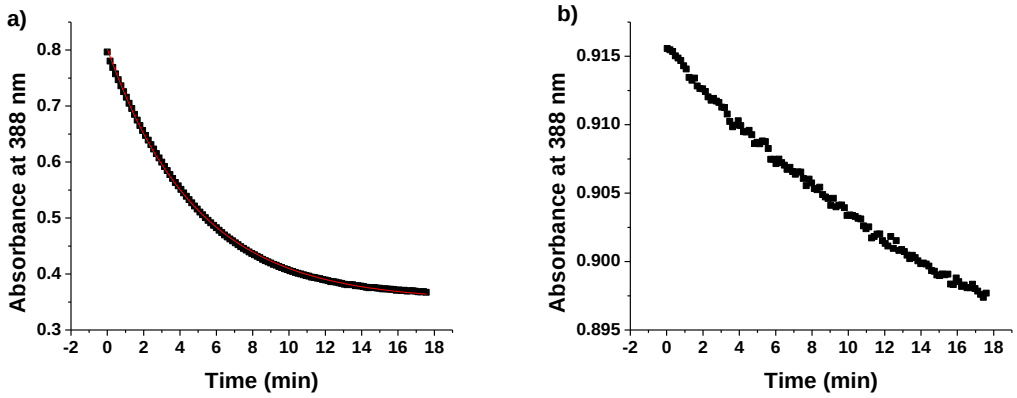

Figure 11: (a) Kinetic data showing the change in absorbance at 388 nm versus time for the reaction of Cbl(I) (50 μM) with NO_2^- (5.0 mM) (0.050 M CAPS buffer, pH 10.80, *I* = 0.50 M (Na_2HPO_4)). Fitting the data to equation (2) gives $k_{obs} = 0.209 \pm 0.001\ s^{-1}$. (b) Plot of absorbance versus time for Cbl(I) (50 μM, same conditions) at pH 10.80 showing the oxidation to Cbl(II) in buffer alone over the same period of time.

The dependence of the rate of the reaction on NO_2^- concentration can be determined by measuring the observed rate constant as a function of NO_2^- concentration for a given pH condition. The reaction order with respect to NO_2^- is determined by plotting k_{obs} versus NO_2^- concentration, as shown in Figure 12. The slope of each plot represents the apparent rate constant (k_{app}) at a given pH value. The linear relationship between k_{obs} and NO_2^- concentration is indicative of the first-order dependence of the reaction rate on NO_2^- concentration.

Under acidic pH conditions (pH 6.50 and 6.92), Cbl(I) was not stable enough to proceed with kinetic measurements by mixing a solution of Cbl(I) in buffer with NO_2^- in buffer. Collection of the Cbl(I) UV-Vis spectrum after dilution in acidic biological buffer (BIS-TRIS and MES) showed partial oxidation to Cbl(II). Therefore, the Cbl(I) solution

was instead prepared in water and only combined with the buffer within the stopped-flow spectrophotometer. The plots of k_{obs} versus NO_2^- concentration had significant intercepts for acidic pH conditions.

The acid dependence for the reaction between Cbl(I) and NO_2^- can be determined from the relationship between k_{app} and the pH. Figure 13 and Table 12 summarize the dependence of k_{app} on pH. The data fit an exponential decay function

$$k_{app} = k10^{-pH} \quad (3)$$

At each pH condition

$$rate = k_{app}[Cbl(I)][NO_2^-] \quad (4)$$

The pH-dependent rate law is

$$rate = k[Cbl(I)][NO_2^-][H^+] \quad (5)$$

Therefore, $k_{app} = k[H^+] = k10^{-pH}$. Fitting the k_{app} versus pH data to equation (3) (Figure 13) gives $k = (1.7 \pm 0.1) \times 10^{10}\ M^{-2}s^{-1}$ for the third-order rate equation (5).

Physiological pH is 7.4. Substituting this into equation (5) yields a second-order rate law at pH 7.4

$$rate = k_1[Cbl(I)][NO_2^-] \quad (7)$$

where $k_1 = (6.6 \pm 0.5) \times 10^2\ M^{-1}s^{-1}$. As the pH decreases, the rate constant is expected to increase according to the model used. The rate of the reaction was not investigated near the pK_a of HNO_2 (pK_a 3.16[46]) because the reaction at pH values less than 6.50 was too fast to be measured using stopped-flow spectrophotometry. As the pH increases, the rate approaches 0, as seen in Figure 13. This suggests that the reactive species is HNO_2

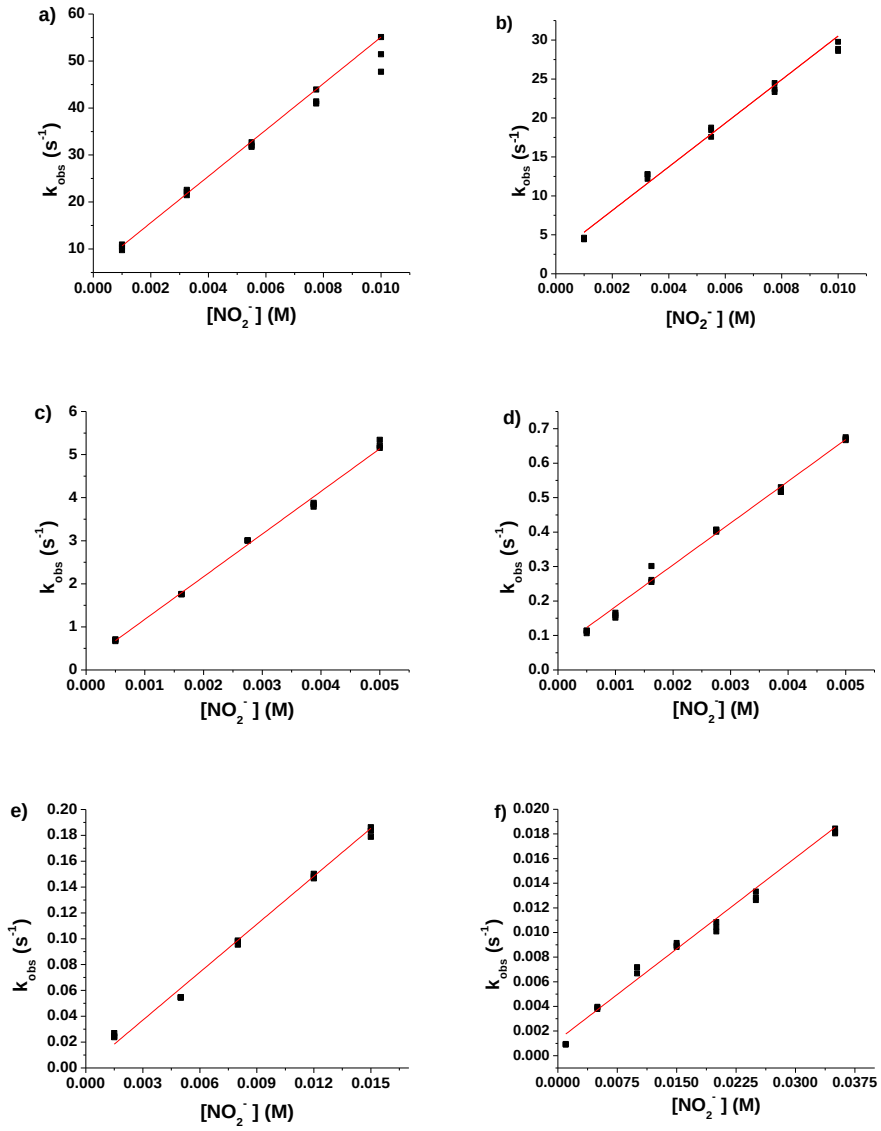

Figure 12: Plot of k_{obs} versus $NaNO_2$ concentration (25.0 °C, I = 0.50 M NaH_2PO_4 / Na_2HPO_4) for (a) pH 6.50 (0.050 M MES), (b) pH 6.92 (0.050 M BIS-TRIS), (c) pH 7.40 (Na_2HPO_4), (d) pH 8.51 (0.050 M TAPS), (e) pH 9.51 (0.050 M CHES), and (f) pH 10.80 (0.050 M CAPS). Linear regressions were performed on the data at each pH. The slopes (k_{app} in $M^{-1}s^{-1}$) were found to be (a) (4.94 ± 0.04) x 10^3, (b) (2.8 ± 0.1) x 10^3, (c) (9.9 ± 0.3) x 10^2, (d) (1.21 ± 0.07) x 10^2, (e) 12.4 ± 0.5, and (f) 0.49 ± 0.02, respectively. The intercepts (in s^{-1}) were found to be (a) 5.7 ± 0.3, (b) 2.5 ± 0.8, (c) 0.2 ± 0.1, (d) 0.06 ± 0.02, (e) no intercept, (f) (1.3 ± 0.4) x 10^{-3}, respectively.

instead of NO_2^-. HNO_2 is a stronger oxidant ($E(HNO_2/N_2)$ = 1.45 V, pH 0; $E(NO_2^-/N_2)$ = 0.41 V, pH 14 versus SHE[42]) due to electron-withdrawing effects of the acidic proton. Substituting the equilibrium expression and the K_a for HNO_2 in the rate law given in equation (7) gives a rate law expressed in terms of HNO_2:

$$\text{rate} = k_2[\text{Cbl(I)}][HNO_2] \quad (8)$$

where $k_2 = (1.15 \pm 0.08) \times 10^7\ M^{-1}s^{-1}$.

Table 12: Apparent rate constants (k_{app}) and intercepts of the plots for the reaction of Cbl(I) with NO_2^- as a function of pH (25.0 °C, I = 0.50 M NaH_2PO_4 / Na_2HPO_4).

pH	k_{app} ($M^{-1}s^{-1}$)	Intercept (s^{-1})
6.50	4940 ± 40	5.7 ± 0.3
6.92	2800 ± 100	2.5 ± 0.8
7.40	990 ± 30	0.2 ± 0.1
8.51	121 ± 7	0.06 ± 0.02
9.51	12.4 ± 0.5	0
10.80	0.49 ± 0.02	0.0013 ± 0.0004

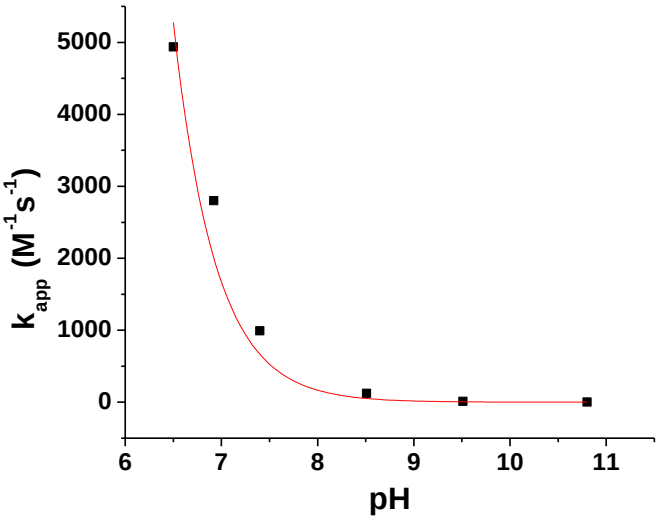

Figure 13: Plot of k_{app} versus pH. The data was fitted to equation (3) in the text, giving $k = (1.7 \pm 0.1) \times 10^{10}\ M^{-2}s^{-1}$.

Figure 14 gives a plot of the intercept of the k_{obs} versus NO_2^- plots (Figure 12) for the reaction between Cbl(I) and NO_2^- at each pH condition. The intercepts are indicative of a second reaction competing with the Cbl(I) + NO_2^- reaction. Figure 14 shows that the rate of the second reaction increases with decreasing pH. For pH 6.92 and 6.50, it was found that decomposition of Cbl(I) to Cbl(II) is significant during the time periods of the reaction. It was assumed that the process would occur within five half-lives derived from the intercepts of the k_{obs} versus NO_2^- concentration plots; that is, within 1.4 s at pH 6.92 and within 0.61 s at pH 6.50. Although the fit of the Cbl(I) decomposition to a first-order equation was poor, as a first approximation, the data was fitted to the first-order kinetics equation (2). At pH 6.92, the average rate constant was 2.4 ± 0.2 s^{-1} in agreement with the intercept value of 2.5 ± 0.8 s^{-1}. At pH 6.50, the average rate constant was 3.9 ± 0.7 s^{-1} compared with the intercept value of 5.7 ± 0.3 s^{-1}. The results for pH 6.50 were more

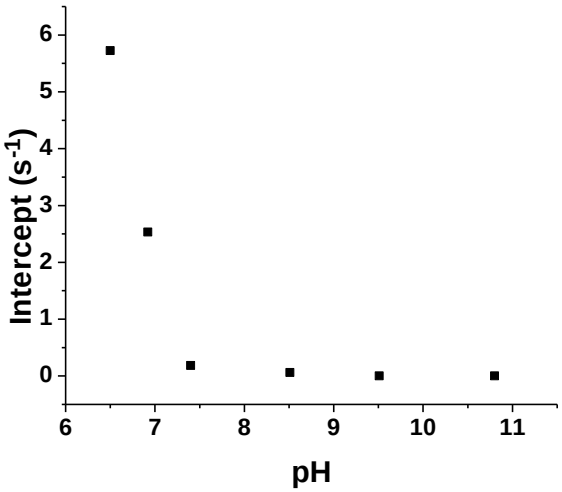

Figure 14: Plot of the intercepts from the k_{obs} versus NO_2^- plots (Figure 12) versus pH. The intercepts at pH 7.40 and higher are insignificant, but the intercepts in acidic pH are significant.

variable and appeared to be experiment-dependent. The observation of this process supports the hypothesis that Cbl(I) oxidation to Cbl(II) competes with the reaction of Cbl(I) with NO_2^- under acidic pH conditions. This reaction is most likely attributable to the reduction of H^+ by Cbl(I) to give H_2 and Cbl(II). The reduction potential of H^+ to give H_2 is 0 V by definition of the SHE, and the reduction potential of the Cbl(II)/Cbl(I) redox couple is -0.600 V versus SHE.[20] Therefore, the cell potential (E_{cell}) is 0.600 V and, the formula

$$\Delta G = -nFE_{cell} \quad (9)$$

where n is the number of electrons involved in the redox process and F is the Faraday constant, (F = 96,485 $Cmol^{-1}$) allows computation of the Gibbs free energy (ΔG). The ΔG is negative (ΔG = -232 kJ/mol), indicative of a spontaneous process. Acid dependent decomposition of Cbl(I) has also been reported by others.[47]

A mechanism can be proposed for the reaction between Cbl(I) and NO_2^- based on the complete balanced equation (1) and the kinetic data. Cbl(I) can be oxidized by HNO_2 to Cbl(II) by a $1e^-$ process or to hydroxocobalamin HOCbl by a $2e^-$ process. Scheme 3(a) outlines the $1e^-$ process, and Scheme 3(b) outlines the $2e^-$ process.

The rate-determining step of the $1e^-$ process (Scheme 3(a)) results in reduction of HNO_2 to $^{\bullet}NO$, and the subsequent reaction (equation (11)) of Cbl(I) with $^{\bullet}NO$ has been studied by others.[48] The subsequent reaction of the mechanism is also known,[49] and gives N_2 as the final product. This reaction pathway does not produce the experimentally observed NH_2OH and gives a stoichiometry of 3:1 Cbl(I):HNO_2 instead of the experimentally determined 4:1 stoichiometry. Thus, Scheme 3(a) can be ruled out.

a) $2H^+ + 2Cbl(I)^- + 2HNO_2 \xrightarrow{\text{slow, } 1e^-} 2Cbl(II) + 2^{\bullet}NO + 2H_2O$ (10)

$2H^+ + 2Cbl(I)^- + 2^{\bullet}NO \xrightarrow{\text{fast}} 2Cbl(II) + N_2O + H_2O$ (11)

$2H^+ + 2Cbl(I)^- + N_2O \xrightarrow{\text{fast}} 2Cbl(II) + N_2 + H_2O$ (12)

$6H^+ + 6\ Cbl(I)^- + 2HNO_2 \longrightarrow 6\ Cbl(II) + N_2 + 4H_2O$ (13)

b) $(2)H^+ + Cbl(I)^- + HNO_2 \xrightarrow{\text{slow, } 2e^-} HOCbl^+ + (H)NO + H_2O$ (14)

$(2)3H^+ + Cbl(I)^- + (H)NO \xrightarrow{\text{fast}} HOCbl^+ + NH_2OH$ (15)

$2Cbl(I)^- + 2HOCbl^+ \xrightarrow{\text{fast}} 4Cbl(II)$ (16)

$4H^+ + 4Cbl(I)^- + HNO_2 \longrightarrow 4Cbl(II) + NH_2OH + H_2O$ (17)

Scheme 3: Postulated reaction pathways for the reaction between Cbl(I) and HNO_2. (a) gives the pathway for a $1e^-$ rate-determining step and (b) gives the pathway for a $2e^-$ rate-determining step.

The rate-determining step of the $2e^-$ process (Scheme 3(b)) results in reduction of HNO_2 to HNO. HNO is an oxidizing agent and is reduced to NH_2OH.[50] The reduction potential of HNO, $2H^+$ / NH_2OH is 0.3 V versus SHE at pH 7,[51] making it a moderate oxidizing agent capable of oxidizing Cbl(I) (E(Cbl(II)/Cbl(I)) = -0.600 V versus SHE[20]). Thus equation (15) is thermodynamically feasible. Alternatively, N_2O rather than HNO could be produced in the first step of this pathway, but others have shown that N_2O reacts with Cbl(I) to give N_2,[49] which was not the experimentally observed product. Finally, the first step in Scheme 3(b) (equation (14)) must be the slow step of the process because there is no observed accumulation of the HOCbl intermediate. Figure 6(a) shows clean and complete conversion of Cbl(I) to Cbl(II), so equations (15) and (16) must be rapid compared to equation (14). Importantly, the rate constant for the reaction of Cbl(I) with

Cbl(III) is 3.2×10^{7} $M^{-1}s^{-1}$,[49] which is significantly larger than the second-order rate constant for the reaction of Cbl(I) and NO_2^- at pH 7.4 (6.6×10^{2} $M^{-1}s^{-1}$).

IV. CONCLUSIONS

The stoichiometry, reaction products, and the kinetics of the reaction of Cbl(I) with NO_2^- have been determined. The Cbl product of the reaction was identified as Cbl(II) by UV-Vis spectrophotometry. Stoichiometry experiments showed that 0.25 mole equiv. of NO_2^- is required for the reaction to proceed to completion. Thus, Cbl(I) and NO_2^- react in a 4:1 mole ratio. The non-Cbl reaction product was determined to be NH_2OH as suggested by the reaction stoichiometry and the indooxine test for NH_2OH. The amount of indooxine product formed did not quantitatively account for the expected amount of NH_2OH produced according to the reaction stoichiometry, but control experiments showed that the Cbl(II) reaction product catalyzes the disproportionation of NH_2OH in solution. Bubbling oxygen through the solution before doing the indooxine test recovers some of the NH_2OH, although full recovery could not be achieved. The complete balanced equation for the reaction is

$$4H^+ + 4Cbl(I)^- + HNO_2 \longrightarrow 4Cbl(II) + NH_2OH + H_2O \quad (18)$$

The kinetics of the reaction between Cbl(I) and NO_2^- were studied under pseudo-first-order conditions as a function of pH. Each reactant was found to exhibit first-order dependence with respect to its concentration. The rate law of the reaction for Cbl(I) with NO_2^- was found to be

$$\text{rate} = k[Cbl(I)][NO_2^-][H^+] \quad (19)$$

The rate constant, k, is $(1.7 \pm 0.1) \times 10^{10}$ $M^{-2}s^{-1}$. Under physiologically relevant conditions

(pH 7.4), the rate expression becomes

$$\text{rate} = k_1[\text{Cbl(I)}][NO_2^-] \quad (20)$$

where $k_1 = (6.6 \pm 0.5) \times 10^2\ M^{-1}s^{-1}$ for the second-order process. The reactive species is thought to be HNO_2, so the rate law can also be expressed as

$$\text{rate} = k_2[\text{Cbl(I)}][HNO_2] \quad (21)$$

where $k_2 = (1.15 \pm 0.08) \times 10^7\ M^{-1}s^{-1}$ at pH 7.4. It has been determined that the source of the intercepts in the plots of k_{obs} versus NO_2^- concentration under acidic pH conditions is acid catalyzed decomposition of Cbl(I) to Cbl(II).

The mechanism of the reaction was determined to be as follows:

$$(2)H^+ + \text{Cbl(I)}^- + HNO_2 \xrightarrow{\text{slow}} HOCbl^+ + (H)NO + H_2O \quad (22)$$

$$(2)3H^+ + \text{Cbl(I)}^- + (H)NO \xrightarrow{\text{fast}} HOCbl^+ + NH_2OH \quad (23)$$

$$2\text{Cbl(I)}^- + 2HOCbl^+ \xrightarrow{\text{fast}} 4\text{Cbl(II)} \quad (24)$$

$$4H^+ + 4\text{Cbl(I)}^- + HNO_2 \longrightarrow 4\text{Cbl(II)} + NH_2OH + H_2O \quad (25)$$

Tissue NO_2^- concentrations are as high as 10 μM[8,15] under normal conditions and may be significantly elevated during periods of cellular oxidative and nitrosative stress. The total Cbl concentration in cells is 30-700 nM in humans,[52] which is significantly lower than the concentration of NO_2^-. Cbl(I) itself is a transient species present at very low concentrations. To give perspective, the NO_2^- concentration (10 μM) can be substituted into the rate law in equation (20) to give

$$\text{rate} = k_3[\text{Cbl(I)}] \quad (26)$$

where $k_3 = (6.6 \pm 0.5) \times 10^{-4}\ s^{-1}$ for the first-order process. The half-life, $t_{1/2}$, for the reaction at pH 7.4 with 10 μM NO_2^- is therefore estimated to be 17 min. Under periods of

oxidative / nitrosative stress, the NO_2^- concentration will be significantly higher, and the half-life therefore shorter.

Both mammalian B_{12}-dependent enzymes are oxidized under oxidative and nitrosative stress conditions.[53] Thus, Cbl(I), while bound to the B_{12} enzymes or B_{12} transport proteins, is still accessible to rapidly react with small ROS and RNS including NO_2^-. Cbl(I) is formed as a precursor to the formation of the two B_{12} cofactors CH_3Cbl and AdoCbl in addition to its role as a transient intermediate in the methionine synthase reaction.[20] The B_{12}-dependent enzyme reactions are known to be deactivated under periods of oxidative and nitrosative stress.[33] This study has shown that the reaction of Cbl(I) with HNO_2 most likely results in deactivation the Cbl(I) intermediate in the metabolically important methionine synthase and MMCM reactions.

REFERENCES

(1) Agarwal, A.; Gupta, S.; Sharma, R. *Reproductive Biology and Endocrinology* **2005**, *3*, 28.

(2) Wasim Khan, M.; Naqshbandi, A.; Zubair, H.; Ahsan, H.; Khan, S.; Khan, F. *The Protein Journal* **2010**, *29*, 276.

(3) Reifenberger, M. S.; Arnett, K. L.; Gatto, C.; Milanick, M. A. *American Journal of Physiology - Renal Physiology* **2008**, *295*, F1191.

(4) Dong M, S. Y., Cheng Q, Hao M *J Reprod Med* **2001**, *46*, 887.

(5) Rosselli, M.; Keller, R.; Dubey, R. *Human Reproduction Update* **1998**, *4*, 3.

(6) Vega, M.; Johnson, M.; Díaz, H.; Urrutia, L.; Troncoso, J.; Devoto, L. *Endocrine* **1998**, *8*, 185.

(7) Ignarro, L. *Nitric Oxide: Biology and Pathobiology*,; Academic Press: San Diego, **2000**.

(8) Heinecke, J.; Ford, P. C. *Coordination Chemistry Reviews* **2010**, *254*, 235.

(9) Avery, A. A. *Environmental Health Perspectives* **1999**, *107*, 583.

(10) Misonou, Y.; Asahi, M.; Yokoe, S.; Miyoshi, E.; Taniguchi, N. *Nitric Oxide* **2006**, *14*, 180.

(11) Zunic, G.; Pavlovic, R.; Malicevic, Z.; Savic, V.; Cernak, I. *Nitric Oxide* **2000**, *4*, 123.

(12) G. Zunic, P. R., M. Vuceljic, O. Jovanikic *Vojnosanit. Pregl.* **2005**, *62*, 273.

(13) Zunic, G.; Colic, M.; Vuceljic, M. *Nitric Oxide* **2009**, *20*, 264.

(14) Kelm, M. *Biochimica et Biophysica Acta (BBA) - Bioenergetics* **1999**, *1411*, 273.

(15) Oplander, C.; Suschek, C. V. *J Invest Dermatol* **2009**, *129*, 820.

(16) Wong, H. R.; Carcillo, J. A.; Burckart, G.; Shah, N.; Janosky, J. E. *Critical Care Medicine* **1995**, *23*, 835.

(17) Rassaf, T.; Feelisch, M.; Kelm, M. *Free Radical Biology and Medicine* **2004**, *36*, 413.

(18) Gonzalez, F. M.; Shiva, S.; Vincent, P. S.; Ringwood, L. A.; Hsu, L.-Y.; Hon, Y. Y.; Aletras, A. H.; Cannon, R. O., III; Gladwin, M. T.; Arai, A. E. *Circulation* **2008**, *117*, 2986.

(19) Hogenkamp, H. C. P. In *Chemistry and Biochemistry of B12*; Banerjee, R., Ed.; John Wiley & Sons: New York, **1999**, p 3.

(20) L. Randaccio, S. G., N. Demitri, J. Wuerges *Molecules* **2010**, *15*, 3228.

(21) Kräutler, B. *Biochemical Society Transactions* **2005**, *33*, 806.

(22) Davies, M. B. *Coordination Chemistry Reviews* **1993**, *124*, 107.

(23) S. Rothenberg, E. Q., A. Regec In *Chemistry and Biochemistry of B12*; Banerjee, R., Ed.; John Wiley & Sons: New York, **1999**.

(24) Kalra, S.; Ahuja, R.; Mutti, E.; Veber, D.; Seetharam, S.; Scalabrino, G.; Seetharam, B. *Archives of Biochemistry and Biophysics* **2007**, *463*, 128.

(25) Birch, C. S.; Brasch, N. E.; McCaddon, A.; Williams, J. H. H. *Free Radical Biology and Medicine* **2009**, *47*, 184.

(26) N. L. Reynaert, K. C., E. F. Wouters, A. van der Vliet, Y. M. Janssen-Heininger *Antioxid Redox Signal* **2005**, *7*, 139.

(27) Schulman, I.; Zhou, M.-S.; Raij, L. *Current Hypertension Reports* **2005**, *7*, 61.

(28) Hsieh, Y.-Y.; Chang, C.-C.; Tsai, F.-J.; Lin, C.-C.; Chen, J.-M.; Tsai, C.-H. *Molecular Human Reproduction* **2004**, *10*, 713.

(29) Schrier, R. W.; Wang, W. *New England Journal of Medicine* **2004**, *351*, 159.

(30) Valko, M.; Rhodes, C. J.; Moncol, J.; Izakovic, M.; Mazur, M. *Chemico-Biological Interactions* **2006**, *160*, 1.

(31) M. A. Erkurt, İ. A., N. Bayraktar, İ. Kuku, E. Kaya *Turk. J. Hematol.* **2009**, *26*, 197.

(32) E. Hazneci, A. B. K., Ç. Öztürk, K. Batçioğlu, G. Doğan, Ş. Karaca, M. Eşrefoğlu *International Journal of Dermatology* **2005**, *44*, 636.

(33) Padovani, D.; Banerjee, R. *Biochemistry* **2009**, *48*, 5350.

(34) Brown, K. L.; Hakimi, J. M.; Nuss, D. M.; Montejano, Y. D.; Jacobsen, D. W. *Inorganic Chemistry* **1984**, *23*, 1463.

(35) Zenon Schneider, A., Stroiński *Comprehensive B12*; Walter de Gruyter: Berlin, **1987**.

(36) Barker, H. A.; Smyth, R. D.; Weissbach, H.; Toohey, J. I.; Ladd, J. N.; Volcani, B. E. *Journal of Biological Chemistry* **1960**, *235*, 480.

(37) J. S. Stamler, D. R. A. In *Methods in Nitric Oxide Research*; J. S. Stamler, M. F., Ed.; John Wiley & Sons: New York, **1996**.

(38) P. Arne Hansen, V. N. *Journal of Biological Chemistry* **1939**, *131*, 309.

(39) Schrauzer, G. N.; Deutsch, E.; Windgassen, R. J. *Journal of the American Chemical Society* **1968**, *90*, 2441.

(40) Motwani, H. V.; Fred, C.; Haglund, J.; Golding, B. T.; Tornqvist, M. *Chemical Research in Toxicology* **2009**, *22*, 1509.

(41) Balasubramanian, P. N.; Gould, E. S. *Inorganic Chemistry* **1983**, *22*, 2635.

(42) Holleman, A. F. In *Inorganic Chemistry*; Wiberg, N., Ed.; Academic Press: San Diego, **2001**, p 657.

(43) Morgan, T. D. B.; Stedman, G.; Hughes, M. N. *Journal of the Chemical Society B: Physical Organic* **1968**, 344.

(44) Alluisetti, G. E.; Almaraz, A. E.; Amorebieta, V. T.; Doctorovich, F.; Olabe, J. A. *Journal of the American Chemical Society* **2004**, *126*, 13432.

(45) Bari, S. E.; Amorebieta, V. T.; Gutiérrez, M. M.; Olabe, J. A.; Doctorovich, F. *Journal of Inorganic Biochemistry* **2010**, *104*, 30.

(46) da Silva, G.; Kennedy, E. M.; Dlugogorski, B. Z. *The Journal of Physical Chemistry A* **2006**, *110*, 11371.

(47) Pratt, J. M. *Inorganic Chemistry of Vitamin B12*; Academic Press: New York, **1972**.

(48) Zheng, D.; Yan, L.; Birke, R. L. *Inorganic Chemistry* **2002**, *41*, 2548.

(49) Blackburn, R.; Kyaw, M.; Swallow, A. J. *Journal of the Chemical Society, Faraday Transactions 1: Physical Chemistry in Condensed Phases* **1977**, *73*, 250.

(50) Jackson, M. I.; Han, T. H.; Serbulea, L.; Dutton, A.; Ford, E.; Miranda, K. M.; Houk, K. N.; Wink, D. A.; Fukuto, J. M. *Free Radical Biology and Medicine* **2009**, *47*, 1130.

(51) Shafirovich, V.; Lymar, S. V. *Proceedings of the National Academy of Sciences of the United States of America* **2002**, *99*, 7340.

(52) Banerjee, R.; Gherasim, C.; Padovani, D. *Current Opinion in Chemical Biology* **2009**, *13*, 484.

(53) Fedosov, S. N.; Fedosova, N. U.; Nexø, E.; Petersen, T. E. *Journal of Biological Chemistry* **2000**, *275*, 11791.